Brain Graphs: Graphical Models of the Human Brain Connectome

Edward T. Bullmore[1] and Danielle S. Bassett[2]

[1]Behavioural & Clinical Neuroscience Institute, Department of Psychiatry, University of Cambridge, Cambridge Biomedical Campus, Cambridge CB2 0SZ, United Kingdom; email: etb23@cam.ac.uk

[2]Department of Physics, University of California, Santa Barbara, Santa Barbara, California 93106

Annu. Rev. Clin. Psychol. 2011. 7:113–40

First published online as a Review in Advance on December 3, 2010

The *Annual Review of Clinical Psychology* is online at clinpsy.annualreviews.org

This article's doi:
10.1146/annurev-clinpsy-040510-143934

548-5943/11/0427-0113$20.00

Keywords

network, systems, topological, connectome, connectivity, neuroimaging

Abstract

Brain graphs provide a relatively simple and increasingly popular way of modeling the human brain connectome, using graph theory to abstractly define a nervous system as a set of nodes (denoting anatomical regions or recording electrodes) and interconnecting edges (denoting structural or functional connections). Topological and geometrical properties of these graphs can be measured and compared to random graphs and to graphs derived from other neuroscience data or other (nonneural) complex systems. Both structural and functional human brain graphs have consistently demonstrated key topological properties such as small-worldness, modularity, and heterogeneous degree distributions. Brain graphs are also physically embedded so as to nearly minimize wiring cost, a key geometric property. Here we offer a conceptual review and methodological guide to graphical analysis of human neuroimaging data, with an emphasis on some of the key assumptions, issues, and trade-offs facing the investigator.

Contents

WHAT IS A BRAIN GRAPH? 114
WHY BOTHER WITH BRAIN GRAPHS AS MODELS OF THE HUMAN BRAIN CONNECTOME? 114
Generalizability 114
Interpretability 116
Clinical Relevance 117
Caveats 117
HOW TO CONSTRUCT A BRAIN GRAPH 118
What Is a Node? 118
What Is an Edge? 120
MEASURES ON GRAPHS 127
Topological Measures 127
Geometric Measures 129
COMPARING AND VISUALIZING BRAIN GRAPHS 130
Comparing Graphs 130
Visualizing Graphs 131
BEYOND THE SIMPLEST GRAPHS 131
Directional Connections and Causal Relationships 131
Weighted Network Analysis 132
CONCLUSIONS 133

WHAT IS A BRAIN GRAPH?

Graph: a model of a complex system completely defined by a set of nodes or vertices and the edges or lines drawn between them; mathematical theory of random graphs originated with Euler and later Erdös and Renyi in the 1950s. Analysis of nonrandom graphs has grown rapidly as an aspect of complexity science in the past 20 years

A brain graph is a model of a nervous system as a number of nodes interconnected by a set of edges. For example, the edges can represent functional or structural connections between cortical and subcortical regional nodes based on analysis of human neuroimaging data. Once a brain graph has been constructed by defining the nodes and edges, its topological properties can be measured by a rich array of metrics that has been developed recently in the field of statistical physics of complex networks (Albert & Barabási 2002) and historically built on the concepts of graph theory (Erdös & Rényi 1959). Since the nodes of a brain graph can be spatially localized, or physically embedded, its geometrical properties can also be estimated and potentially related to network topology.

To date, most such human brain graphs have specified binary connectivity—the edges between nodes are undirected and unweighted; see **Figure 1**. The construction of such binary brain graphs is the focus of this article, although we also briefly describe the construction of directed and/or weighted brain graphs.

WHY BOTHER WITH BRAIN GRAPHS AS MODELS OF THE HUMAN BRAIN CONNECTOME?

Brain graphs are simple models of the real underlying connectome (Sporns et al. 2005). They are properly based on a number of more-or-less explicit, and more-or-less realistic, technical assumptions. For example, we will usually assume that the nodes are independent and internally coherent, and we may also assume that all the edges signify the same strength of connection between nodes. Such assumptions inevitably entail some loss of information in the resulting graphs compared to the multivariate datasets from which they were constructed. However, the technical constraints and robust simplifications of graph theoretical analysis, applied to human neuroimaging data, are worth it—arguably—for two strategic reasons: generalizability and interpretability.

Generalizability

Graph theoretical analysis is potentially applicable to any scale, modality, or volume of neuroscientific data (Bassett & Bullmore 2006, Bullmore & Sporns 2009, Sporns, 2010). We can say this with some confidence because graph theory has already proven to be applicable to a considerable diversity of complex systems, including markets, ecosystems, computer circuits, and gene-gene interactomes (Barabási 2009). Some of these systems have been graphically modeled on a much bigger scale than has so far been attempted for nervous systems. For example, graph models have

been constructed for the World Wide Web comprising up to 200 million nodes (Websites) and 1.5 billion edges (links) (Barabási & Albert 1999, Broder et al. 2000); and for the brain gene transcriptome, comprising up to 20,000 nodes, each representing expression of genetically specific mRNA, with each edge representing significant coexpression of mRNA related to a pair of genes (Oldham et al. 2006). Thus, graph theory potentially provides a common language for the analysis of complex systems in general, and we expect to be able to use it to describe some of the key topological properties of nervous systems from the cellular scale of the neuronal connectome, exemplified by that of the nematode worm, *Caenorhabditis elegans*, to the whole-brain scale of human neuroimaging data.

Within the domain of human brain mapping, graph models have now been reported for all major modalities of magnetic resonance imaging (MRI) and neurophysiological data. Functional brain graphs have been constructed from functional MRI (fMRI) (Achard & Bullmore 2007, Achard et al. 2006, Eguíluz et al. 2005, Liu et al. 2008, Salvador et al. 2005a, van den Heuvel et al. 2008), electroencephalography (EEG) (Micheloyannis et al. 2006, Stam et al. 2007a), and magnetoencephalography (MEG) data (Bassett et al. 2006, Deuker et al. 2009, Stam 2004). Structural brain graphs have been constructed from diffusion tensor imaging (DTI) or diffusion spectrum imaging (DSI) (Gong et al. 2008, Hagmann et al. 2008) and conventional MRI data (Bassett et al. 2008, He et al. 2007). This degree of generalizability immediately supports comparison of topological parameters between structural and functional networks. For example, it has been discovered that fMRI and DTI brain graphs consistently demonstrate some common global topological properties (Honey et al. 2009, Park et al. 2008, Skudlarski et al. 2008, Zalesky & Fornito 2009; see **Figure 1**), including:

- small-worldness—indicating a balance between network segregation and integration,
- modularity—indicating a decomposability of the system into smaller subsystems, and
- heterogeneous degree distributions—broad-scale or fat-tailed probability distributions of degree, indicating the likely presence of network hubs or highly connected nodes.

It is conceptually easier to link the brain graphs derived from these different data types to each other than it would be if each imaging dataset were described in terms of some modality-specific measure of association between regions, e.g., tractographic connection probabilities from DSI or correlations between regional fMRI time series. Facilitating between-modality translation of results can be important for methodological cross-validation and, more fundamentally, for informing our understanding of how functional networks might interact with the substrate of a relatively static structural network (Honey et al. 2009).

The generalizability of graph theory also allows us to compare the topological properties of large-scale or macro networks represented by neuroimaging to those of small-scale or cellular networks measured by microscopy or microelectrode recording. This is potentially important in defining organizational properties of nervous systems that are conserved across scales of space and time, and across different species. More radically, the generalizability of graph theory encourages the translation of new ideas from analysis of nonneural complex systems, such as principles of high-performance microprocessor design, to quantification of the human brain connectome (Bassett et al. 2010). We can thus begin to address questions such as, what is special about the human connectome compared to a variety of other complex, information-processing systems? Do human brain networks represent a singular pinnacle of organizational complexity or are they one of a universality class of superficially diverse networks that share important topological properties in common? These questions about conservation of topological principles across

Topology: spatial properties that are invariant under continuous deformation are topological aspects of a system. In brain graphs, topological analysis considers the connectivity between nodes regardless of their physical or anatomical locations

Connectivity: a measure of association between neurons or brain regions. In human neuroimaging, functional connectivity means that two regions demonstrate similar dynamics over time, whereas effective connectivity means that one region has a causal effect on dynamics in another region

Degree: the degree of a node is the number of edges connecting it to the rest of the network; the distribution of degrees over all nodes in the network can be described as a degree (probability) distribution. Brain graphs typically have a broad-scale degree distribution, implying that at least a few "hub" nodes will have high degree

Small-worldness: originally defined as the combination of high clustering and short characteristic path length; subsequently also defined as the combination of high global and local efficiency of information transfer between nodes of a network

Modularity: modular networks are those that are composed of topological modules or communities. A module is defined as a group of nodes that have many connections to other nodes within the module but few connections to nodes outside the module

Cost: a topological definition of the cost of a system is the number of edges in proportion to the total number of possible edges; a physical definition weights the cost by the geometric distance between nodes. Brain networks economize (but do not minimize) both topological and physical costs

Efficiency: a word with many meanings but usually understood as a measure of information transfer between nodes; a network with high global efficiency will have a short characteristic path length. Cost-efficiency relates the efficiency of the graph to its cost or connection density

information-processing systems are potentially important because topological conservation suggests that diverse systems have convergently evolved to satisfy universal optimization criteria. The identity and interdependence of such putative network selection criteria are not yet fully established, but plausible candidates include minimization of wiring cost (a geometric measure of physical distance between connected nodes), maximization of efficiency of information transfer (a topological measure inversely related to path length between nodes), hierarchical modularity, and high dimensional interconnect topology (Bassett et al. 2010, Robinson et al. 2009). Through the prism of graph theory, we can begin to test ideas about evolution and development of human brain networks that are informed by what we know about the selection of many other, perhaps experimentally more tractable, networks.

Interpretability

Biological and behavioral interpretability is always an issue in human neuroimaging. The anatomical and physiological significance of structural and functional MRI signals has been extensively debated but not yet entirely resolved (Lee et al. 2010, Lerch et al. 2006). Imaging studies of brain systems or networks inevitably depend on some measure of signal association or covariation between regions, but the neurobiological basis is not yet settled for either interregional correlations in brain structure estimated over subjects in MRI or interregional correlations in brain function estimated over time in fMRI. Lacking a clear structural or physiological substrate for changes in anatomical or functional connectivity, measured by statistical association between regions at the systems level of neuroimaging, it is difficult to predict how changes in such descriptive statistics should be related to cognitive or behavioral performance of the system. For example, is it cognitively "good" or "bad" to have a greater-than-average correlation between a pair of fMRI time series representing, say, left middle frontal gyrus and right hippocampus? Similarly, it is difficult to explain why specific neuropsychiatric disorders, e.g., schizophrenia, have often been associated with a profile of both abnormally increased and decreased magnitude of connectivity across different brain regions (Rubinov et al. 2009, Whitfield-Gabrieli et al. 2009). Is less connectivity always a sign of the disease process, and more connectivity in a patient group always a sign of a compensatory process, or can excess connectivity be directly pathological?

The translation of modality-specific connectivity statistics to topological measures on brain graphs may help us to find more secure cognitive and clinical interpretations of neuroimaging systems. This proposition is far from proven yet, although there are some encouraging early signs in its favor. For example, three recent studies—using fMRI (van den Heuvel et al. 2009), MEG (Bassett et al. 2009), and DTI (Li et al. 2009)—have independently reported associations between general intelligence or executive task performance and topological measures of brain network efficiency or cost-efficiency. In general, higher cognitive performance has been associated with brain graphs globally configured for greater efficiency—speed and fidelity—of parallel information transfer between regional nodes. This observation is compatible with neuropsychological theories that higher-order cognitive functions depend on distributed processing (Fodor 1983) across a large, integrated "neuronal workspace" (Dehaene & Naccache 2001): A network with higher global efficiency will be more optimized as a cognitive workspace. There have also been early reports that disease-related changes in topological properties of brain graphs can be related to other aspects of the disorder in question. For example, reductions in network efficiency have been associated with greater white matter lesion load in patients with multiple sclerosis (He et al. 2009a), and reductions in nodal degree (the number of edges connecting a regional node to the rest of the brain graph) have been associated with

greater severity of local amyloid deposition in patients with Alzheimer's disease (Buckner et al. 2009). It is also notable that moderate levels of heritability have been reported for brain graph topology measured in a twin study using EEG (Smit et al. 2008), suggesting that there may be important genetic effects on variation in brain graph metrics. Collectively, these and other early results suggest that it will be interesting to apply graph theory more extensively to the cognitive, clinical, and genetic interpretation of neuroimaging systems.

Clinical Relevance

The organization of brain graphs is modulated by an array of factors that varies throughout the healthy population, including behavioral variability (Bassett et al. 2009), cognitive ability (Li et al. 2009, van den Heuvel et al. 2009), shared genetic factors (Smit et al. 2008), genetic information (Schmitt et al. 2008), age (Meunier et al. 2008, Micheloyannis et al. 2009), and gender (Gong et al. 2009). The architecture of an individual's connectivity is inherently dynamic, being altered by experimental tasks (Bassett et al. 2006, de Vico Fallani et al. 2008a) and drug treatment (Achard & Bullmore 2007, Schwarz et al. 2009).

Complex network theory is particularly appealing when applied to the study of clinical neuroscience, where many cognitive and emotional disorders have been characterized as dysconnectivity syndromes (Catani & ffytche 2005), as indicated by abnormal phenotypic profiles of anatomical and/or functional connectivity between brain regions. For example, in schizophrenia, a profound disconnection between frontal and temporal cortices has been suggested to characterize the brain (Friston & Frith 1995); in contrast, people with autism may display a complex pattern of hyperconnectivity within frontal cortices but hypoconnectivity between the frontal cortex and the rest of the brain (Courchesne & Pierce 2005). In fact, a wealth of clinical and disease states have recently been shown to manifest themselves by abnormal cortical graph organization: schizophrenia (Bassett et al. 2008, 2009; Liu et al. 2008; Lynall et al. 2010; Micheloyannis et al. 2006; Rubinov 2009), Alzheimer's disease (He et al. 2008, 2009a; Stam 2010; Stam et al. 2007a; Supekar et al. 2008), epilepsy (Horstmann et al. 2010, Raj et al. 2010, van Dellen et al. 2009), multiple sclerosis (He et al. 2009b), acute depression (Leistedt et al. 2009), absence seizures (Ponten et al. 2009), medial temporal lobe seizures (Ponten et al. 2007), attention deficit hyperactivity disorder (Wang et al. 2010), stroke (de Vico Fallani et al. 2009, Wang et al. 2009), spinal cord injury (de Vico Fallani et al. 2008b), fronto-temporal lobar degeneration (de Haan et al. 2009), and early blindness (Shu et al. 2009). Together, these studies highlight the extended clinical relevance of graphical analysis of human neuroimaging data.

Caveats

So far we have emphasized the attractive simplicity, generalizability, interpretability, and clinical relevance of brain graphs. Now we return to our major caveat: graph analysis of neuroimaging data is not "plug and play." It is a model building exercise, entailing arbitrary assumptions and decisions, which can have influential effects on the results of the analysis. It is also relativistic: Many of the results from a brain graph will need to be calibrated by comparison to the extreme bounds of random and regular graphs (see **Figure 1**), e.g., to quantify small-worldness of the brain networks, or we may wish to compare one group of brain graphs to another. How best to compare topological metrics between graphs is not a trivial question. In addition to these relatively specialist questions about construction and comparison of brain graphs, any approach to systems analysis of neuroimaging data also raises a number of issues about data acquisition and preprocessing, statistical hypothesis testing and multiple comparisons, visualization, etc. In what follows, we attempt to address some of these caveats in greater detail.

HOW TO CONSTRUCT A BRAIN GRAPH

The two key questions to address in constructing a graphical model of a brain network are, (*a*) What is a node, and (*b*) What is an edge?

What Is a Node?

Before we describe the previously used definitions of nodes in neuroscience and neuroimaging, it is important to describe what properties a node should have in general (Butts 2009). In graphical models, a node is a portion of the system that is separable from the other portions of the system in some way; i.e., nodes are meant to be inherently independent or distinct in the system under study. To put it another way, the interactions between nodes will become continuously less meaningful the more similar the nodes are to each other. In addition to being independent, the nodes should be internally coherent or homogeneous, i.e., nodes should be encapsulated informational components that have internal integrity and external independence (Butts 2008, 2009; Rubinov & Sporns 2010).

Cellular systems. A cellular nervous system has an immediately obvious graphical deconstruction: each neuron can be considered an independent and homogeneous node, and the synapses between neurons can be considered as edges. This is the intuitively straightforward basis for the graphical analysis of the cellular connectome of the nematode worm, *C. elegans* (Bassett et al. 2010, Watts & Strogatz 1998), which comprises about 300 cellular nodes and about 7,600 synaptic edges. It has also been the basis for graphical modeling of small-world cellular networks in vertebrate brainstem (Humphries et al. 2006). However, we note that *C. elegans* is currently the only organism for which the cellular connectome has been completely described; graphical modeling of cellular connectomes in other species will be challenged by their greater size and variability, and even in this most tractable case, graphical analysis involves making choices about whether all types of neurons should have equal status as nodes [more than 100 classes of neurons are recognized in *C. elegans* (White et al. 1986)].

Electrophysiological data. For graphical analysis of neurophysiological data on electromagnetic fields, including microelectrode recordings from cortical tissue (Yu et al. 2008) as well as scalp electrode recordings in EEG or surface sensors in MEG, it may be reasonable to define each electrode or signal sensor as a node. Defining nodes as MEG or EEG sensors will preserve the native covariance structure of the data, but without appropriate preprocessing (Stam et al. 2007b), this will include strong correlations between neighboring sensors due to volume conduction of electrical activity from a single source in the brain to multiple nearby electrodes or sensors on the scalp surface. In graphical terms, untreated volume conduction will be represented by a regular lattice-like structure of highly clustered connections between spatially neighboring sensors, which could clearly confound analysis of brain network properties such as small-worldness.

An alternative approach is to reconstruct the sensor data in terms of anatomically located sources and define each source as a node (Palva et al. 2010a,b). This allows the operator some discretion in how many nodal sources should be reconstructed from a fixed number of sensors, and it deals with the issue of volume conduction. However, it is also important to bear in mind that some source reconstruction algorithms, such as the synthetic aperture magnetometry beamformer, solve the inverse problem by diagonalizing the sensor covariance matrix to render sources as statistically independent from each other (see, e.g., Cheyne et al. 2006). This is obviously unlikely to represent an optimal starting point for an analysis of functional connectivity between sources. Other reconstruction algorithms assume stationarity (constant mean and variance over time) of the time series, which is unlikely to be realistic over the duration of a typical experimental recording (from

tens to thousands of seconds) (Kowalik & Elbert 1994).

Thus we can see that a preprocessing step (source reconstruction) that might seem attractive for defining the nodes of an MEG network could have severe effects on the covariance between nodes that will later be used to define the edges of the network (Vrba & Robinson 2001). Most graphical studies of neurophysiological data so far have used sensors as nodes (Bassett et al. 2006, 2009; Stam 2004, 2010), implicitly sacrificing anatomical resolution and independence of nodes for greater data fidelity of edges representing covariation between nodes. This trade-off has not been extensively studied in terms of its impact on statistical properties of graph metrics derived from neurophysiological data. It seems clear from preliminary work that headline properties of human brain functional networks—such as small-worldness and broad-scale degree distributions—are qualitatively conserved whether network nodes are defined as sources (Palva et al. 2010b) or sensors (Deuker et al. 2009), but this is an area where there is likely to be further significant methodological development in the future.

Tract-tracing and MRI data. For graphical analysis of tract-tracing data on large-scale axonal projections between regions of mammalian cortex, nodes have usually been defined cytoarchitectonically as Brodmann areas (Hilgetag et al. 2000; Scannell et al. 1995, 1999; Young 1992, 1993). In some of the early graphical studies of human neuroimaging data, an approximately equivalent convention was followed to define nodes (Achard et al. 2006, Bassett et al. 2008, Wang et al. 2008). Each individual's brain image was coregistered with an anatomically parcellated template image, and the mean signal over all voxels in each region of the template image was taken as the nodal value at that anatomical location. Several similar but not identical template images are available (see Related Resources) and have been used for this purpose. It has been shown that use of different anatomical templates for analysis of the same imaging data can lead to subtly different graphical results (Wang et al. 2010). It has also been suggested by analysis of simulated fMRI data that specification of functionally, rather than anatomically, defined nodes may improve fidelity of functional network modeling (Smith et al. 2010).

The main advantage of using an anatomically defined template for nodal parcellation of neuroimaging data is that it can support direct comparison of results to prior neuroimaging or primate neuroanatomy studies using the same or a similar template. The main disadvantage, which is probably more significant, is that the size of different template regions can vary considerably. For fMRI analysis, for example in the Automated Anatomical Labeling (AAL) template (Tzourio-Mazoyer et al. 2002) (**Figure 2**), the middle frontal gyrus region comprises many more voxels than the hippocampus region. Nodal values obtained by averaging across many voxels in larger regions will be less noisy than nodal values estimated by averaging across smaller regions, leading to a bias in favor of stronger statistical associations between larger regions of the template image (Salvador et al. 2008). One way of dealing with this bias is to randomly sample the same number of voxels in estimation of each nodal value, but this is likely to mean that larger nodes are less internally coherent.

An increasingly preferred approach to definition of nodes in fMRI data has been to stipulate that each node should comprise an equal number of voxels and that nodes should collectively cover the brain without prior anatomical information being used to guide their size or location (Zalesky et al. 2010b). If this approach is adopted, the key parameter to choose is the spatial size of each node, which can range from a minimum of 1 voxel to a maximum in the order of 10^4 voxels. We can see immediately that each spatial scale represents a trade-off between the defining nodal properties of independence and coherence: Single voxel nodes will be more coherent but less independent of each other (to the extent that the image is spatially smooth), whereas larger nodes, located regardless of

approximate cytoarchitectonic fields, will be less coherent but more independent.

There has been limited systematic exploration of the effect of nodal size on overall network properties. A few fMRI studies adopting the minimum nodal size of one voxel have reported scale-free or power law degree distributions of the resulting networks (Eguíluz et al. 2005, van den Heuvel et al. 2008), whereas the majority of fMRI and MRI studies using anatomical templates with larger nodes have reported exponentially truncated power law degree distributions (e.g., Achard et al. 2006). This indicates that some network properties, such as the form of the degree distribution, may be qualitatively affected by the size of the nodes—in this case, voxel nodes leading to networks with a larger probability of very highly connected hubs. It is not yet clear whether this apparent difference in degree distributional properties as a function of the spatial scale of network nodes reflects a biological difference in network organization at different spatial scales or the reduced independence of voxel nodes that are small compared to the spatial smoothness of the image. However, a study of anatomical networks derived from the same set of DTI and DSI data as nodal size was continuously increased from small nodes, comprising a local cube of $\{3 \times 3 \times 3\}$ voxels, to large nodes, comprising $\{100 \times 100 \times 100\}$ voxels, found that the form of the degree distribution and other topological properties were quite consistently expressed across scales, although the quantitative values of topological parameters were scale dependent (Zalesky et al. 2010b).

Another factor to take into consideration when deciding the size of nodes is that smaller nodes will naturally be more numerous, and hypothesis testing of nodal statistics, e.g., to produce a cortical surface map of between-group differences in nodal degree, will require a larger number of statistical tests and therefore more stringent multiple comparisons corrections. In other words, the greater spatial resolution of local network properties conferred by smaller nodes comes at the cost of more conservative significance thresholds to control type I (false positive) error in the context of multiple comparisons. This is a familiar trade-off in the context of mass univariate statistical testing for classical brain activation mapping.

What Is an Edge?

We have seen that there is no absolutely correct or straightforward answer to the question of defining nodes. The question of how to define edges in a brain graph is even more open to a variety of legitimate choices. As before, the case of *C. elegans* can provide a deceptively simple template: The edges in this cellular connectome are usually defined as the synapses between neurons, which are highly reliable between different worms and have been exactly described (White et al. 1986). But should electrical and chemical synapses be given equal weight as edges? Should the directionality of chemical synapses be respected by specification of directed edges in the corresponding graph? In practice, most graphical analyses of *C. elegans* have adopted the simplest possible choice—all synaptic connections are represented as undirected and unweighted (or equally weighted) edges—but this is clearly not the only possible choice. When we turn to the graphical analysis of neuroimaging, neurophysiological, and other data where we lack a "ground truth" knowledge of the physical connections between nodes, a reasonable specification of edges becomes more challenging.

To explore the methodological issues in this context, we consider the illustrative example of building a graph model for the human functional connectome based on a single fMRI dataset (see **Figure 2*A***). Several questions immediately arise; e.g., under what experimental conditions should the data be recorded, and how should they be preprocessed prior to graph analysis? To date, most graph models of fMRI data have been based on data recorded with participants lying quietly in the scanner, at rest. However, there is no reason in principle why graphs could not be constructed from data recorded while subjects

perform experimentally controlled cognitive tasks; indeed, this strategy is likely to become more popular in the future, as attention focuses on the question of how graphical parameters of functional network organization can be related to cognitive performance (see Future Issues and Palva et al. 2010a for an example of task-related network analysis using MEG).

For resting-state data analysis, one common question is how long a functional MRI time series should be to support investigation of functional associations and networks. From a strictly technical point of view, a larger number of time points will generally improve the precision of time series model parameter estimates. The frequency bandwidth of a digital time series process is limited by the Nyquist frequency ($f_N = f_S/2$, where f_S is the sampling frequency) at the upper end and by the length of the time series at the lower end ($f_{\min} = 1/T$, where T is the number of time points in the series). Within these limits, higher-frequency components will generally be estimated with greater precision than low-frequency components (Achard et al. 2008). In fMRI, interest is often focused on a low-frequency range <0.1 Hz, which is considered to be more purely representative of neuronal (noncardiorespiratory) sources of (co)variation, and the sampling interval is typically on the order of seconds. These considerations indicate that fMRI time series will ideally be recorded over at least 5 to 10 minutes (Van Dijk et al. 2010), and longer time series (about 30 minutes) have been reported (Achard et al. 2006). However, very long periods of fMRI recording may be difficult for subjects to tolerate without excessive head movement or changes in brain state such as falling asleep. In general, basing functional connectivity or network analysis on very long periods of time series, although technically preferable, incurs the assumption that brain functional systems are in the same (stationary) state over the period of observation, which becomes increasingly implausible as the length of observation increases. The assumption of stationarity also arises if several short segments of fMRI time series, e.g., the resting-state epochs of a classical blocked periodic activation paradigm, are concatenated to form a composite time series for connectivity and network analysis (Fair et al. 2007). This procedure assumes that the brain is in approximately the same functional state before and after performance of cognitive tasks, although there is some evidence that endogenous brain dynamics recorded immediately after effortful task performance may be different from the dynamics preceding task performance (Barnes et al. 2009).

In addition to the question of time series length, there are multiple preprocessing steps commonly applied in fMRI analysis that will likely have as yet incompletely characterized effects on functional brain graphs. For example, nodal time series are often corrected for head movement and for other "nuisance covariates," such as global brain or white matter mean fluctuations, before estimation of association metrics (Poldrack et al. 2008). Such preprocessing steps can significantly alter the specificity, strength, and localization of measured functional associations and therefore may substantially alter the topology of brain graphs derived from the association matrices (Murphy et al. 2009, Van Dijk et al. 2010, Weissenbacher et al. 2009).

However, many of these issues concerning data acquisition and preprocessing are generic to fMRI studies of brain functional connectivity and are not uniquely problematic from the perspective of graph analysis. To focus more specifically on the issues arising in graph analysis, we use a representative single fMRI dataset (results shown in **Figure 2*A***), acquired over the course of about 37 minutes (equivalent to 2,048 time points at each voxel) from a healthy volunteer in the resting state. The data were preprocessed to correct voxel times series for head movement and slice timing offsets, then regionally parcellated using the AAL template (Tzourio-Mazoyer et al. 2002), which defines 90 cortical and subcortical regions; methodological details are described in Achard et al. (2006). Thus, the dataset available for graph analysis comprised a $\{N \times T\}$ or $\{90 \times 2048\}$ multivariate time series (see **Figure 2*A***).

Association matrix: a matrix of connectivity measures between each possible pair of the nodes in the system; applying a global threshold to an association matrix to generate a binary adjacency matrix is the simplest and most frequently used approach to graph analysis of human neuroimaging data

Functional association. Given a multivariate time series like an fMRI dataset (or an MEG or EEG or MEA recording), the first significant choice we have to make is how to describe the statistical association between each nodal time series. In general, we estimate the pair-wise association $a_{i,j}$ between the ith and jth nodes, $i \neq j = 1, 2, 3, \ldots, N$ and compile these statistics for all possible pairs in a $\{N \times N\}$ interregional association matrix, A (see **Figure 2*A*,*B***). Many measures of association could be used for this purpose, and they can be categorized by various criteria. Following Friston (1994), we can distinguish measures of functional connectivity, such as correlation coefficients, from measures of effective connectivity, such as path coefficients. A functional connectivity statistic measures the extent to which two processes behave similarly over time; an effective connectivity statistic measures the extent to which one process can be predicted or explained by the other. Thus, the association matrix generated by estimating the functional connectivity between each pair of nodes will be symmetric, whereas the association matrix generated by an effective connectivity analysis need not be. To date, almost all graphical analyses of fMRI data have been based on a symmetric association matrix generated by some measure of functional connectivity between nodes; however, there is no reason in principle why methods of effective connectivity analysis, such as path analysis or dynamic causal modeling, could not be used as the statistical basis for a functional brain graph.

Moreover, this distinction between functional and effective connectivity, although influential, does not exhaust the ways in which various association measures can be distinguished (David et al. 2004). Some measures of functional connectivity, such as the correlation coefficient, will only capture linear interactions between time series, whereas other measures, such as the mutual information (Bassett et al. 2009), phase synchronization (Kitzbichler et al. 2009, Palva et al. 2010a), or synchronization likelihood (Stam 2004), are sensitive to both linear and nonlinear interactions. Some measures are sensitive to association between nodal time series subtended by a specific frequency interval, such as the wavelet correlation (Bullmore et al. 2004) or coherence in the frequency domain (Salvador et al. 2005b). Some measures, such as the partial correlation (Salvador et al. 2005a) or partial coherence (Salvador et al. 2005b), are particularly sensitive to the specific association between each pair of nodes and will discount third-party effects, such as shared inputs from a third node or global mode of covariation.

We cannot offer definitive guidance about which of these or other possible association statistics is "best" for the purposes of graph analysis [though see David et al. (2004) and Smith et al. (2010) for evaluation of multiple possible connectivity metrics in the context of simulated data]. But we can offer some general suggestions about how to deal with this moment of choice. First, it is wise to bear in mind the nature and limitations of the data, and the hypothetical question of interest. In our illustrative example, we have a resting state fMRI data matrix where the number of time points (2,048) is about one order of magnitude greater than the number of nodes (90). Under these circumstances, it is probably advisable to start with a simple measure of stationary association, especially if focusing on a low-frequency interval, e.g., $\leq$0.1 Hz, to mitigate nonneuronal contributions to covariation between nodes. If the time series were longer, it might be more attractive to look at dynamic or nonstationary aspects of association; if the number of nodes was smaller relative to the number of time points, more sophisticated measures of association such as dynamic causal modeling might be computationally tractable; if the data had been acquired during performance of multiple discrete cognitive trials, rather than at rest, it might be interesting to measure the correlation of event-related response amplitude between nodes (Yoon et al. 2008).

Whichever measure of association is chosen, our second piece of general advice would be to look at the association matrix carefully before proceeding to graphical analysis (**Figure 3*A*,*B***). Several simple exploratory analyses may

be informative and will build a preliminary understanding of the data before they are more abstractly represented by a graphical model. For example, it may be useful to calculate the grand mean of the association matrix and, for each node, its mean association with the rest of the matrix: we refer to these as measures of the strength of association. The mean strength of association for the *i*th node is simply $\bar{a}_{i,.} = \frac{1}{N}\sum_j a_{i,j}$. It may also be useful to consider the between-node variation in strength of association and the within-node variation of association to all other nodes in the system: We can refer to these as measures of the diversity of association. It can also be informative to use principal component (PC) analysis to identify major modes of covariation between multiple nodes; for example, the ratio of the first eigenvalue, λ_1, to the sum of other eigenvalues can provide a measure of the global integration of the system $I = \frac{\lambda_1}{\sum_2^N \lambda_j}$ (Lynall et al. 2010, Tononi et al. 1994). Many other exploratory multivariate techniques could be used at this stage.

The basic idea is to get acquainted with the association matrix in relatively simple terms before it is transformed to an adjacency matrix and described topologically. Such an incremental approach will generally prevent us from thinking about the results of graphical analysis as the output of a "black box" procedure and will likely be predictive of some of the key topological results. For example, the most highly connected nodes or hubs of a brain graph will typically be those nodes with the highest mean strength of connectivity (**Figure 4**). The value of preliminary exploratory analysis is particularly clear when we are dealing with several individual association matrices representing brain systems in subjects drawn from different patient groups or studied under different experimental conditions (see below).

Structural association. Conceptually identical approaches can be taken to the graphical analysis of structural networks derived from measures of anatomical connectivity between nodal regions. Anatomical connectivity can be defined in different ways, based on different kinds of MRI data. For diffusion tensor or spectrum imaging, it is possible to assign a probability of axonal connection between any pair of gray matter regions on the basis of tractographic analysis of an individual dataset. For conventional (e.g., T1-weighted) MRI data, anatomical connectivity has been inferred by thresholding a matrix of interregional covariation in cortical thickness or volume of multiple regions (Bassett et al. 2008, He et al. 2007) (see **Figure 2*C***). Strong between-subject covariation in local gray matter measurements has been interpreted as indicative of axonal connectivity between covarying regions, on the grounds that connectivity has mutually trophic effects on the growth of connected neurons or regions, leading to correlations in the size of the regions when they are measured after a period of development (Mechelli et al. 2005, Wright et al. 1999). This is not the only possible interpretation—as noted, the cellular substrates for many neuroimaging phenomena are unresolved—but there is some empirical evidence that regions with high gray matter covariation measured in conventional MRI also have a high probability of being connected by axonal projections inferred from tractographic analysis of DTI or DSI data (Lerch et al. 2006).

Both MRI and DT/SI-based anatomical networks have their limitations. The main drawback of MRI-based anatomical connectivity analysis, besides the question of its cellular substrate, is that it depends on covariation over individual subjects. Precise estimation therefore demands MRI data, ideally on hundreds of subjects, to yield a single association matrix, and thus a single network, for the whole group. This precludes analysis of how individual differences in anatomical network organization might be associated with other individual differences, such as variability in performance of a cognitive task. In contrast, the main advantage of DT/SI-based anatomical connectivity analysis, in addition to its more clearly defined cellular substrate, is that an association matrix can be estimated for each subject, where $a_{i,j}$

denotes the connection probability between regions *i* and *j* estimated by some tractography algorithm (Hagmann et al. 2008, Iturria-Medina et al. 2007). This allows investigators to explore associations between measures on individual anatomical networks and other individually variable measures, such as functional networks derived from fMRI, or cognitive variables such as IQ scores or executive function, or clinical variables such as white matter lesion load in patients with multiple sclerosis.

The main current disadvantage of DT/SI-based networks is that tractography on available data seems generally to underestimate the probability of connections between regions that are a long distance apart in the brain. This is because long-distance projections are more likely to intersect with other, differently orientated projections, and it is more difficult to trace the course of a single tract in the context of crossing fibers. More recent acquisition sequences, such as the HARDI sequence for DSI, have been shown to generate networks with a higher probability of long-distance connections than older, classical DTI sequences (Zalesky et al. 2010b). Foreseeable improvements in diffusion data acquisition and analysis tools can be expected to produce high-quality anatomical networks in single subjects.

Thresholding and connection density. Having thus estimated an association matrix from the data, the next crucial question is, what kind of graph do we wish to construct from the association matrix? We will continue to illustrate possible solutions in relation to a functional association matrix based on our illustrative fMRI dataset, but many of the issues apply directly to graphical analysis of other association matrices. As already noted, most investigators using fMRI for this purpose to date have estimated a measure of functional connectivity between nodes, such as the correlation coefficient, and then thresholded the resulting association matrix A to create a binary adjacency matrix $\mathcal{A}$ (**Figure 5**). We can describe this more formally by saying that a threshold τ is applied to each element $a_{i,j}$ of the association matrix, and if $a_{i,j} \geq \tau$, the corresponding element of the adjacency matrix $\alpha_{i,j}$ is set to unity; otherwise, if $a_{i,j} < \tau$, $\alpha_{i,j} = 0$. If there is a nonzero element in the adjacency matrix, this is equivalent to saying there is an unweighted and undirected edge between the corresponding nodes of the network. In other words, the thresholding operation on the association matrix will define the edges in the adjacency matrix and will therefore have a strong influence on the topology of the network. So a key subsidiary question that arises is, what should be the value of the threshold τ?

Let's consider the limiting cases first, initially assuming for the sake of simplicity that the association between each pair of nodal time series has been described in terms of the absolute correlation coefficient $0 \leq |a_{i,j}| \leq 1$. If $\tau = 0$, then all elements of the association matrix will pass the threshold, all elements of the adjacency matrix will be nonzero, all possible edges in the graph will exist, and the connection density of the graph κ will be maximized. We can generally define the connection density or topological cost of the graph as

$$0 \leq \kappa \leq 1 = \frac{\mathcal{E}_\tau}{\frac{N(N-1)}{2}}, \qquad (1)$$

where $\mathcal{E}_\tau$ is the number of edges generated by thresholding at some value of τ, and $\frac{N(N-1)}{2}$ is the maximum number of edges that could exist in a network of N nodes. Clearly, when $\tau = 0$, $\kappa = 1$. It should also be clear that if $\tau = 1$ in this case, then no elements of the association matrix will pass the threshold, all elements of the adjacency matrix will have the value of zero, there will be no edges in the graph, and its connection density will be zero. The important generalization is that if the threshold is set below the minimum value of the association matrix, the adjacency matrix will have maximum connection density, whereas if the threshold is set above the maximum value of the association matrix, the adjacency matrix will have minimum connection density, and as the threshold is gradually increased from minimum

to maximum values, this will result in monotonically, but not necessarily linearly, decreasing connection density of the graph (**Figure 5**). Thus, we can describe any threshold on any association measure in terms of the connection density or topological cost of the resulting graph, and this will always fall in the range $0 \leq \kappa \leq 1$ (Stam et al. 2007a). We will see that this translation from threshold value τ to connection density κ is useful, but it does not yet answer the question of which threshold(s) to apply.

There are two broad approaches to thresholding: We can search for a single, in some sense optimal, threshold to apply to each association to decide if it should be an edge and describe the topological properties of the resulting network only at that threshold (Achard et al. 2006, He et al. 2007), or we can threshold the association matrix at many different values and describe the resulting network properties as a function of changing threshold or connection density (Achard & Bullmore 2007, Bassett et al. 2008).

One way to define a single threshold is by controlling the probability of type I (false positive) error on multiple hypothesis testing of each element in the association matrix. For example, in our illustrative example, we have 4,050 unique elements of the association matrix. We could set τ such that $\text{Prob}(a_{i,j} > \tau) \leq 0.05$, which will result in about 200 bidirectional nonzero elements in the adjacency matrix under the null hypothesis. More conservatively, we could set τ so as to control the expected number of false positives, or the false discovery rate (Genovese et al. 2002, He et al. 2007). These are both examples of mass bivariate hypothesis testing, where a statistical hypothesis is tested independently for each of a large number of bivariate measures of association between nodes. An alternative approach may be to apply a preliminary statistical threshold to each edge and then test the null hypothesis at the level of suprathreshold clusters of interconnected edges (Zalesky et al. 2010a). This is akin to the use of cluster-level statistics in classical fMRI activation mapping (Bullmore et al. 1999), although in this case clusters of edges are defined topologically rather than clusters of voxels being defined by spatial proximity, as in the classical case.

Our preference has been to explore network properties as a function of changing threshold. As the threshold is gradually relaxed, more edges are added to the network, so it becomes increasingly dense or less sparsely connected (see **Figure 4**). The complex or nonrandom topology of brain graphs is typically clearest in relatively low-cost networks, i.e., those with connection densities less than about 0.5. In this first half of the possible cost range, increasing connection density is associated with a disproportionate increase in global and local efficiency of network topology, and the small-world properties of the system are most clearly demonstrated by comparison to random networks (**Figure 6**). The greater-than-linear increase in efficiency as a function of cost means that the cost-efficiency difference is typically positive and has a maximum value at connection density about 0.3 (Achard & Bullmore 2007, Bassett et al. 2009) (see **Figure 6**). At lower thresholds, associated with connection densities greater than 0.5, the law of diminishing returns seems to apply. Addition of extra edges, or increasing connection cost, is associated with relatively modest increments of network efficiency; small-world properties are less clearly delineated; and the networks become indistinguishable from random graphs at highest connection costs.

This behavior allows us to define a small-world cost regime as the range of connection densities over which the network exhibits the small-world characteristic: a clustering coefficient greater than the clustering coefficient of a random network and a path length about the same as the path length of a random network (Humphries et al. 2006, Watts & Strogatz 1998); for mathematical definitions, see the following section on Measures on Graphs: Topological Measures. This definition of small-worldness clearly requires that the experimental

Clustering: a measure of the cliquishness of connections between nodes in a topological neighborhood of the graph; the nearest neighbors of a highly clustered node will also be the nearest neighbors of each other. Related to local efficiency and fault-tolerance of the network

network be compared to random networks and regular lattices (Bassett et al. 2010, Kaiser & Hilgetag 2006, Watts & Strogatz 1998). Each of these benchmark graphs has a different degree distribution; that is, a node in each of these networks will have a different probability of being a highly connected hub. This degree distributional variation could predispose the network to have higher or lower values of a given graph metric, such as the clustering coefficient. It is therefore often useful to assess whether the topological structure present in a brain network under study is due to the degree distribution alone or to additional architectural constraints. Thus, it is common practice to compare brain network properties to both (*a*) a pure random network and (*b*) a random network that has been constructed to retain the identical degree distribution of the brain network under study (Maslov & Sneppen 2002).

When random graphs are constructed over a range of connection densities, it is found that the network becomes fragmented, into a giant connected cluster and a number of smaller islands, at a characteristic critical connection density. Thus, for a random graph to be entirely connected, the mean degree of the N nodes needs to be at least $2 \times \log(N)$, or equivalently, the connection density κ needs to be at least $\frac{(2\log(N))N}{N(N-1)/2}$. We can say that there is a percolation threshold, defined as the lowest connection density at which the graph becomes entirely connected and information can percolate freely throughout the whole system.

When brain graphs are constructed by global thresholding over a range of connection densities, they also tend to become fragmented at lower connection densities (see, e.g., **Figure 4**). The percolation threshold is variable between individuals and data types but is typically in the range $0.1 < \kappa < 0.5$. The fragmentation or percolation properties of networks can be topologically informative in their own right and are also closely related to measures of a network's robustness to random error or targeted attack (Achard et al. 2006, Honey & Sporns 2008, Lynall et al. 2010). But this behavior also alerts us to the fact that sparsely connected networks, which tend to be more complex or less random topologically, will often comprise different numbers of fully connected nodes, and this will need to be controlled when it comes to comparing any topological metric between networks. One simple way of controlling the number of connected nodes is to measure graph metrics only over the range of costs for which all individual graphs are entirely connected (Bassett et al. 2008, Lynall et al. 2010). However, if some of the individual networks have high percolation thresholds, this may force comparison of metrics over a less sparsely connected cost range, where differences from randomness will tend to be less salient.

An alternative to global thresholding for graph construction may help to circumvent some of these issues. For example, a graph can be constructed from the minimum spanning tree (MST) (Hagmann et al. 2008). The MST fully connects N nodes with $N - 1$ edges, with low connection density in the order of N/N^2. This means that the MSTs of any two connectivity matrices will be guaranteed to be entirely connected at sparse connection densities and therefore could support comparison of topological metrics controlled for number of edges and number of connected nodes over a more interesting cost range than global thresholding. However, MSTs are by definition acyclic and will not demonstrate biologically plausible clustering of connections between topologically local nodes. Once the MST has been defined as the "skeleton" of the brain network, it must therefore be grown somehow, e.g., by addition of extra edges that pass a global threshold value, such that graph metrics can be estimated over a full cost range of connection densities, without any change in the number of connected network nodes (Alexander-Bloch et al. 2010). Minimum spanning trees and related methods of graph construction may prove to be advantageous as a technical basis for comparing networks, matched for number of nodes and edges, between different groups or experimental conditions. However, there are likely to be significant future developments

concerning the optimal methods for filtering an association matrix to construct a brain graph.

MEASURES ON GRAPHS

Brain graphs are models of physically embedded information-processing networks. Each node has an anatomical address in physical space and a network role in topological space. The brain as a whole is a high-performance network—with many global topological properties in common with high-performance computer chips, economic markets, and other complex systems—physically embedded as a sulco-gyrally convoluted sheet of processing elements interconnected by a core of white matter cabling.

There are therefore two main classes of measure on brain graphs: topological and geometric. Topological metrics capture the relations between nodes regardless of their physical location—an edge can count identically as an edge whether it connects two locally neighboring nodes or a pair of nodes located far apart from each other; a hub node with many edges, or high degree, will count as a hub wherever it is located. Physical metrics capture the relations between nodes in Euclidean space and will have continuous values in SI units. There is obvious potential interest in understanding the interaction between brain network topology and geometry. There are many methods by which topological and geometric measures could be combined; for example, we can weight topological edges by physical distance between nodes for weighted network analysis. We consider that this topo-physical mapping of brain networks is likely to become of considerable interest in the future, although it has not yet been much developed.

Topological Measures

Because network analysis is based on the mathematical field of graph theory, there is a wealth of previously defined metrics that can be used to characterize the topological architecture of the brain's anatomical or functional connectivity. These are parameters of global network organization, and many of them can also be estimated at the single-node or edge level of the graph (see Rubinov & Sporns 2010 for review).

Degree and degree distribution. Perhaps the simplest topological measure is the degree of a node, k, which is defined as the number of edges emanating from that node. Degree, sometimes called degree centrality, has been used to discriminate between nodes in the system that are well connected, i.e., so-called hubs, and nodes that are less well connected, or nonhubs (see **Figure 1**). Due to their relatively increased connectivity, high-degree nodes are likely to play an important role in the system's dynamics. The probability distribution for nodal degree is the degree distribution of the network. Brain graphs generally have heterogeneous or broad-scale degree distributions, meaning that the probability of a highly connected hub is higher than in a comparable random network (see **Figure 6*C***). Most studies have found that an exponentially truncated power law is the best form of degree distribution to fit to networks based on functional and structural MRI data. Some studies have reported that the degree distribution of fMRI networks follows a power law, which implies that the probability of a highly connected hub is higher than it would be if the degree distribution were exponentially truncated. Different degree distributions imply differences in network growth rules. For example, a power law degree distribution is compatible with growth by a simple preferential attachment rule, whereby each new node is more likely to form connections with existing hubs, and there is no limit to the number of connections a hub can sustain; whereas an exponentially truncated distribution implies that there may also be physical constraints on the number of connections that any single node can sustain. It will be interesting to explore computational models of network growth more extensively in relation to emerging empirical data on brain network degree distributions and other topological properties.

Although degree provides a simple measure of a node's hubness, it is not the only measure of a node's significance for the flow of information through the network. The complementary metric of betweenness centrality describes how many shortest paths between any two nodes in the system must pass through the node in question (Freeman 1977). A brain regional node with high centrality is therefore potentially an information bottleneck because it will be involved in many of the shortest paths between other regions of the whole brain network. Although betweenness centrality is the oldest and perhaps most used centrality measure, closeness centrality, eigenvector centrality, and edge centrality all provide similar but not identical information regarding nodal importance (Lohmann et al. 2010, Sporns et al. 2007). Centrality measures can also be estimated for each edge, as well as for each node, in the network.

Small-worldness and efficiency. The two metrics originally used to characterize the *C. elegans* neuronal system were the clustering coefficient, which is a measurement of the efficiency of local connectivity, and path length, which is a simplified measurement of the global efficiency of information transfer on the network (Watts & Strogatz 1998) (see **Figure 3*C***). As described in a previous section, these two metrics enable us to define the small-world property, in which the network exhibits a clustering coefficient, C, greater than the clustering coefficient of a random network, C_r; a path length, L, about the same as the path length of a random network, L_r; and therefore a small-world scalar $\sigma > 1$ (Humphries et al. 2006, Watts & Strogatz 1998), where

$$\sigma = \frac{\frac{C}{C_r}}{\frac{L}{L_r}}. \qquad (2)$$

It is important to note here that reporting a small-world scalar $\sigma > 1$ is not enough to prove small-worldness; both $\gamma = C/C_r > 1$ and $\lambda = L/L_r \sim 1$ are also required. The reason that the relation $\sigma > 1$ is not enough to prove small-worldness is that it is possible to have regular network structures with large clustering coefficients (for example, giving $\gamma = 3$) but also long path lengths (for example giving $\lambda = 2$), which together provide a σ value greater than 1. In other words, regular-lattice-like networks may have small-world scalars $\sigma > 1$, and so to prove small-worldness, both the γ and λ values need to be reported.

The small-world scalar is dependent on the calculation of a path length, which can be troublesome for networks that contain one or more disconnected nodes. The path length of a disconnected node is infinity (it cannot transfer information to any other node on the network), and so the average path length of a network that contains a disconnected node (such as many fMRI networks at sparse threshold; Achard et al. 2006) will also be equal to infinity. In a complementary formalism, Latora & Marchiori (2001) introduced the global efficiency as an alternative metric of global integration that is inversely proportional to the characteristic path length of the network, thus allowing computation of a finite value for graphs with disconnected nodes (Achard & Bullmore 2007). In addition to the global efficiency, Latora & Marchiori (2001) also defined the local efficiency of each node, which is similar but not equivalent to its clustering coefficient or fault tolerance (see **Figure 3*D***). Subsequently, Achard & Bullmore (2007) defined the nodal efficiency as inversely proportional to the path length of connections between a single node and every other node in the network. It can be seen that there are many metrics that include the word efficiency in their name, and care is required to avoid terminological confusion.

As connection density increases, there will be an increase in global efficiency for any graph: More edges make it easier to get from one node to another, but each extra edge adds a marginal cost to the overall topological cost of the network. In brain graphs, efficiency tends to increase faster than linearly as connection density is increased from zero to about 20%, but at progressively higher costs, the extra advantage in efficiency is less than the incremental cost. This means that the difference between global efficiency and topological cost,

so-called cost-efficiency (Achard & Bullmore 2007, Bassett et al. 2009, Deuker et al. 2009), is generally positive and has a maximum value at a critical connection density, which is somewhat variable between subjects but typically about $\kappa \sim 0.3$. The topological cost-efficiency of brain networks is consistent with their classification as economical small-world networks (Latora & Marchiori 2001, 2003).

Modularity. A brain graph can generally be subdivided or partitioned into subsets or modules of nodes (Chen et al. 2008, Meunier et al. 2008). Finding the mathematically optimal modular decomposition for a brain network is not trivial, and several alternative algorithms have been proposed. In general, the aim is to find the partition that maximizes the ratio of intramodular to intermodular edges. Thus the nodes in any module will be more densely connected to each other than to nodes in other modules (Blondel et al. 2008, Leicht & Newman 2008, Newman 2006). The intramodular degree is a measure of the number of connections a node makes with other nodes in the same module. The participation coefficient is a measure of the ratio of intramodular connectivity to intermodular connectivity for each node (Guimera et al. 2007). These and related metrics can be used to define nodes as "connectors" (with high intermodular connections) or "provincials" (with low intermodular connections). We can see that resolving the modular or community structure of a brain graph is likely to add important information about which anatomical regions or tracts have the most critical topological roles in transmission of information across brain networks. We also know from recent work that brain networks are not only modular at a global scale, they also demonstrate a hierarchical modularity (Meunier et al. 2009) or nested arrangement of modules within modules, which may be advantageous in terms of stability, evolvability, and efficiency of physical embedding of complex networks in general (Bassett et al. 2010, Simon 1962).

Other topological metrics. There is no shortage of topological metrics that could be applied to brain graphs. Here we have summarized only a few of the parameters that have been most extensively investigated in the neuroimaging literature to date. The literature on statistical physics of complex networks is the primary source for many other metrics, tools, and concepts for brain graph analysis (Albert & Barabási 2002, Strogatz 2001). There is also a rapidly growing literature on specialist applications to human neuroimaging and other neurophysiological data (for recent reviews, see Bassett & Bullmore 2006, 2009; Bullmore et al. 2009; Bullmore & Sporns 2009; Hagmann et al. 2010; and Wang et al. 2009). In general, it is worth remembering that many topological metrics will be strongly correlated with each other and with more elementary statistical properties of the data. Different metrics often provide convergent angles on the same aspects of network organization: For example, a more hub-dominated degree distribution was associated with greater clustering of connections in fMRI data (Lynall et al. 2010). It is correspondingly unlikely that any single metric will turn out to be uniquely important in capturing the complexity of human brain networks (Costa et al. 2007).

Geometric Measures

The main geometric measure on a graph is the distance between connected nodes. This is sometimes described for convenience as the wiring length of a connection. In human brain networks based on DTI or fMRI data, most connections have short wiring length, but the probability distribution is heavy-tailed and there is a significant minority of long-distance edges (see **Figure 6*D***). Further analysis has shown that the human brain is economically but not minimally wired, meaning the total wiring cost of the network (the sum of all physical distances between connected nodes) is less than it would be if the same nodes were wired up at random but more than if the nodes were rewired to minimize wiring cost (Chen et al.

2006, Kaiser & Hilgetag 2006). This observation implies that conservation of wiring cost has been positively if not uniquely selected in evolution of large-scale brain networks, and it is compatible with much prior data and analysis indicating that many aspects of brain anatomical organization can be approximated by wiring minimization principles (Attwell & Laughlin 2001, Chen et al. 2006, Kaiser & Hilgetag 2006, Niven & Laughlin 2008).

The distance is usually estimated as the Euclidean distance between regional centroid coordinates in stereotactic space. It might be possible to substitute curvilinear estimates of distance from tractographic modeling of DTI/DSI data in the future. The distance between regions can be used, for example, to weight the edges of the network under study. In this case, we could perform what is called a weighted network analysis, in which the weights of the edges are used in the computation of all graph metrics calculated on the network.

Although for the most part topological and geometric measures have remained separate in network analysis, the interactions between topology and space specifically for spatially embedded systems such as the brain will likely prove interesting in future. One interesting avenue will be to assess the spatial distribution of graph metrics throughout the physical space of the system. This has been done in the context of other more generally spatially embedded systems: The spatial distributions of centrality measures have been used, for example, to study urban street architectures (Crucitti et al. 2006). In addition to studying the spatial distributions of graph metrics, we may be able to apply metrics that inherently blend topological and geometric properties, such as the Rent's exponent. Based on work in the computer science literature and recently applied to human brains, the topo-physical metric known as Rentian scaling has been used to quantify the cost-efficiency of physical connectivity in terms of both wiring and connection complexity (Bassett et al. 2010). It is likely that additional metrics and analysis methods will provide added insight into the complex interaction between network topology and physical placement in the human brain, both functionally and structurally.

COMPARING AND VISUALIZING BRAIN GRAPHS

Comparing Graphs

Brain graph analysis inevitably means making comparisons between networks. For instance, we often want to know if some aspect of brain network organization is nonrandom. This will mean comparing the brain network derived from neuroimaging data to a random network generated by computer simulation of an Erdös-Renyí random graph (Erdös & Rényi 1959). For a given number of nodes, we can generate a large number of random graphs with somewhat variable topology and use the distribution of topological metrics in the random graphs as a point of reference to judge the nonrandomness of the same metrics measured in the neuroimaging data. We may also want to compare brain graphs to minimally wired versions of the same network, or to compare brain graphs between groups of subjects, such as a patients and healthy volunteers. In all these examples of comparing brain graphs, it is important to observe two golden rules (Bollobás 1985): The graphs to be compared must have (*a*) the same number of nodes and (*b*) the same number of edges.

This is because the quantitative values of topological metrics will depend on both the size and connection density of the graphs, and in order to identify topological differences between graphs that specifically point to the difference between groups, it is important to control these general effects before making any quantitative comparisons. To test statistical hypotheses about differences between groups of networks, we would also recommend the adoption of nonparametric techniques, e.g., permutation tests for the difference in topological metrics between two groups of brain graphs. The distributional properties of topological metrics are not well known, and the sample sizes in most neuroimaging experiments are not large, presenting challenges for asymptotic theory. More positively, a computationally intensive approach

to inference by Monte Carlo simulations or data resampling offers substantial advantages in terms of flexibility, precision, and validity of testing that are only discounted somewhat by the costs entailed in greater processing time.

In addition to comparing topological structures of entire graphs, we could focus on subnetworks of graphs that are different between groups. Recent progress in applications of machine learning can be used to uncover unique subgraphs that discriminate between two weighted (sparse or complete) graphs (Richiardi et al. 2010), and permutation testing on topological clusters of connections has proven to be statistically powerful in identification of abnormal subnetworks in fMRI data on people with schizophrenia (Zalesky et al. 2010a). Techniques like these may provide a new avenue for the application of complex network analysis to smaller subsets of whole-brain connectivity profiles.

Visualizing Graphs

Brain graphs can be visualized in real space, as seen in **Figure 6*B***, to show their actual physical structure. In a complementary visualization, brain graphs can be plotted in topological space. For example, nodes can be visualized as close to each other if they are part of the same topologically defined cluster or module and far apart from each other if they are separated by a long path length (see **Figure 6*A***). Also, topological properties taken from these brain graphs can be visualized in anatomical space—so-called topophysical mapping. For example, we can produce cortical surface maps of the degree of cortical nodes, highlighting the anatomical distribution of network hubs (see **Figure 4**). See **Table 1** for available software that can be used to visualize brain graphs.

BEYOND THE SIMPLEST GRAPHS

Directional Connections and Causal Relationships

Network edges may be directed (drawn as arrows) or undirected (drawn as lines). A directed edge makes a claim about the causal relations between nodes, whereas an undirected edge is

Table 1 Available tools for network analysis of brains

Human brain atlases	Software	Site
AAL	WFU PickAtlas	**http://www.fmri.wfubmc.edu/cms/**
Brodmann	MRICRO	**http://www.cabiatl.com/mricro/**
Freesurfer	Freesurfer	**http://surfer.nmr.mgh.harvard.edu/**
Harvard-Oxford	FSL	**http://www.fmrib.ox.ac.uk/fsl/**
LPBA40	LONI	**http://www.loni.ucla.edu/Atlases/**
Reference networks	**Laboratory**	**Site**
C. elegans (N = 131,277)	Kaiser	**http://www.biological-networks.org**
Macaque (N = 95)	Kaiser	**http://www.biological-networks.org**
Macaque (N = 71,47)	Sporns	**http://www.indiana.edu/cortex/**
Macaque Visual (N = 30,32)	Sporns	**http://www.indiana.edu/cortex/**
Cat (N = 95,52)	Sporns	**http://www.indiana.edu/cortex/**
Network Toolboxes	**Language**	**Site**
Matlab BGL	Matlab	
Brain Connectivity Toolbox	Matlab	**http://www.indiana.edu/cortex/**
Brainwaver	R	
Network visualization	**Description**	**Site**
gplot	Matlab	**http://www.mathworks.com/matlabcentral/fileexchange**
Pajek	Closed source	**http://pajek.imfm.si/doku.php**
Caret	Van Essen	**http://brainvis.wustl.edu/wiki/index.php**

agnostic about causality—it is simply a claim about association. The directionality or causality of neuronal interactions is not always easily estimated from data. In the neural system of *C. elegans*, many synaptic connections between cells are electrical (not chemical), and this has usually been modeled as a single undirected edge between neuronal nodes (Kaiser & Hilgetag 2006, Watts & Strogatz 1998). Similarly, most interregional axonal connections in mammalian cortex are reciprocal, and most graphical models of macaque and cat cortex have had undirected edges (Kaiser & Hilgetag 2006, Sporns et al. 2004). In human neuroimaging data, it is currently more difficult to assign directionality to associations between regions, whether measured by structural MRI, DTI, DSI, or fMRI. Most graphs constructed from fMRI data have therefore measured symmetric measures of association or functional connectivity, like simple correlation, partial correlation, mutual information, or synchronization likelihood, and constructed undirected graphs on this basis. However, it is possible to model directional edges (Chen & Herskovits 2007) by using, for example, partial directed coherence (Baccalá & Sameshima 2001), dynamic causal modeling (Friston et al. 2003), structural equation modeling (Büchel & Friston 1997), or Granger causality (Bernasconi & König 1999) as measures of asymmetric association or effective connectivity. To date, however, it is unclear whether it is possible to scale these methods to systems with more than a handful of nodes; for the possibility of such a large-scale analysis using structural equation modeling, see Kenny et al. (2009). Computational models have shown that more complex and biologically plausible dynamics can be generated from directed graphs of brain anatomy based on tract tracing data on primates than can be generated from undirected graphs based on diffusion spectrum imaging data on humans (Knock et al. 2009). It seems likely that further development of data and methods for analysis of directed brain graphs will be a priority for future technical innovation.

Weighted Network Analysis

Although the majority of network studies of neuroimaging data have been performed on binary or unweighted networks, in which each edge has a weight of one and each nonedge has a weight of zero, there has been a growing interest in the use of weighted networks, in which edges may have continuously variable weights (see Rubinov & Sporns 2010 for a recent review and **http://sites.google.com/a/brain-connectivity-toolbox.net/bct** for the Brain Connectivity Toolbox software library, which provides code for many of the metrics). One simple approach to weighted network analysis is to start with a binary network constructed at some cost and then assign a weight $w_{i,j}$ to each edge. The weights could be the physical distance between nodes or the strength of functional connectivity between nodes. Most of the topological metrics available for analysis of binary networks have been generalized for weighted network analysis, so weighting a binary adjacency matrix does not restrict the options for topological analysis, and it does retain more physical information in the graph model. The weighting of brain networks by physical connection distance or wiring cost seems likely to be of interest given the prior evidence that wiring costs are highly economized, if not strictly minimized, in animal nervous systems at many spatial scales. It is likely that future studies will increasingly use DT/SI-based measures of anatomical connection distance between nodes as the weights on anatomical and functional networks.

A more radical approach, sometimes also called weighted network analysis, is to estimate metrics that are analogous to topological metrics on a thresholded graph without applying any threshold to the association matrix. For example, unsupervised learning methods, such as the spin-glass algorithm, can be used to decompose an association matrix into clusters that correspond closely to the modules identified by a topological analysis of the adjacency matrix generated by thresholding the association matrix (Alexander-Bloch et al. 2010). It is likely

that there will be further consideration of approaches to network analysis that do not depend on a thresholding step, but of course one of the benefits of global thresholding is that it will remove a proportion of the noisy or random edges from the graph. Metrics estimated directly on the unthresholded association matrix will generally have lower signal-to-noise ratios than metrics estimated on sparsely thresholded graphs.

CONCLUSIONS

Graph analysis is rapidly growing in popularity as an approach to modeling the complexity of the human brain connectome. The fundamental motivations for graph theory as a method of brain network analysis are its relative simplicity and high degrees of generalizability and interpretability. However, like all other modeling endeavors, the results of brain graph analysis are underpinned by basic assumptions or choices, many of which will represent a tradeoff between competitive criteria. We have tried to elucidate some of the conceptual issues and recent methodological advances that will be relevant to an investigator wanting to use these techniques to analyze neuroimaging or other neuroscientific data. Our hope has been to stimulate informed use and further methodological development of graph theoretical networks as models of the human brain connectome.

SUMMARY POINTS

1. Brain graphs are apparently simple but powerful models of the brain's structural or functional connectome; graphical analysis is applicable to many scales and types of neuroscience data and is interpretable in relation to general principles of complex system organization.
2. Key questions to address in any graphical analysis are, what is a node and what is an edge? In neuroimaging or neurophysiological data, a node will typically be a region of the image, or a sensor or electrode of the recording array, and edges will be defined by thresholding a measure of statistical association between nodes. Many methodological issues attend the specification of both nodes and edges.
3. It is recommended to explore network properties over a range of connection densities or topological costs. Sparsely thresholded networks (with cost less than 20%) demonstrate nonrandom properties such as small-worldness and modularity more saliently and are more likely to be fragmented or not entirely connected.
4. Once a brain graph has been constructed, many topological and geometrical properties can be estimated—early work has focused on broad-scale degree distributions, economical small-worldness and cost-efficiency, and modularity. These and other nonrandom properties of network organization have been found consistently across many different types of neuroscientific data, suggesting that they represent highly conserved general principles of connectome organization.
5. Network analysis is relativistic—brain graphs need to be compared to each other and to benchmark networks. In making comparisons, it is generally advisable to ensure that the connection density and number of entirely connected nodes is equivalent between graphs.
6. Weighted network analysis allows incorporation of more physical data, such as the connection distance between nodes, in the topological analysis of network properties.

FUTURE ISSUES

1. Scale. Early brain graph studies have typically used a few images. With the funding of the National Institutes of Health Human Connectome Project (**http://www.humanconnectomeproject.org**) and the related growth of interest in graphical analysis, we can expect publication of brain graphs based on hundreds or thousands of subjects, allowing more powerful studies of genetic and other causes of variation in brain graph parameters.
2. Causality. It will be necessary to optimize techniques to capture directional interactions between neuronal populations and to model large causal systems as directed brain graphs. Most human brain graph studies to date have assumed undirected edges, which is technically simpler but neglects this biologically important aspect of neural systems.
3. Cognition. Aspects of brain graph topology have been linked to cognitive and behavioral performance, but the relationships between psychological and topological properties of brain networks are likely to be investigated more extensively in the future (for example, by greater consideration of task-related functional neuroimaging data).
4. Biomarkers. The potential utility of graphical metrics as diagnostic markers of neuropsychiatric syndromes will be explored on the basis of larger clinical samples and in relation to various dysconnectivity models of schizophrenia and other disorders likely to result from developmentally perturbed formation of the brain connectome.
5. Network movies. Most graphical analyses have provided a static view of brain functional network organization over several seconds or minutes of observation; however, rapid functional network configuration—or nonstationarity—is theoretically important for adaptivity of cognitive function and may be studied by construction of network movies representing time-resolved change in network architecture.

DISCLOSURE STATEMENT

ETB is employed half-time by GlaxoSmithKline and half-time by the University of Cambridge and is a stockholder in GSK.

LITERATURE CITED

Achard S, Bassett DS, Meyer-Lindenberg A, Bullmore E. 2008. Fractal connectivity of long memory networks. *Phys. Rev. E* 77:036104

Achard S, Bullmore E. 2007. Efficiency and cost of economical brain functional networks. *PLoS Comput. Biol.* 3:e17

Early description of small-world structure in resting state fMRI networks.

Achard S, Salvador R, Whitcher B, Suckling J, Bullmore E. 2006. A resilient, low-frequency, small-world human brain functional network with highly connected association cortical hubs. *J. Neurosci.* 26:63–72

Comprehensive review of the physics of complex networks.

Albert R, Barabási AL. 2002. Statistical mechanics of complex networks. *Rev. Mod. Phys.* 74:47–98

Alexander-Bloch A, Gogtay N, Meunier D, Birn R, Clasen L, et al. 2010. Disrupted modularity and local connectivity of brain functional networks in childhood-onset schizophrenia. *Front. Syst. Neurosci.* 4:147

Attwell D, Laughlin SB. 2001. An energy budget for signalling in the grey matter of the brain. *J. Cereb. Blood Flow Metab.* 21:1133–45

Baccalá LA, Sameshima K. 2001. Partial directed coherence: a new concept in neural structure determination. *Biol. Cybern.* 84:463–74

Barabási AL. 2009. Scale-free networks: a decade and beyond. *Science* 325:412–13

Barabási AL, Albert R. 1999. Emergence of scaling in random networks. *Science* 286:509–12

Barnes A, Bullmore ET, Suckling J. 2009. Endogenous human brain dynamics recover slowly following cognitive effort. *PLoS One* 4:e6626

Bassett DS, Bullmore E, Meyer-Lindenberg A, Weinberger DR, Coppola R. 2009. Cognitive fitness of cost-efficient brain functional networks. *Proc. Natl. Acad. Sci. USA* 106:11747–52

Bassett DS, Bullmore ET. 2006. Small-world brain networks. *Neuroscientist* 12:512–23

Bassett DS, Bullmore ET. 2009. Human brain networks in health and disease. *Curr. Opin. Neurol.* 22:340–47

Bassett DS, Bullmore ET, Verchinski BA, Mattay VS, Weinberger DR, Meyer-Lindenberg A. 2008. Hierarchical organization of human cortical networks in health and schizophrenia. *J. Neurosci.* 28:9239–48

Bassett DS, Greenfield DL, Meyer-Lindenberg A, Weinberger DR, Moore SW, Bullmore ET. 2010. Efficient physical embedding of topologically complex information processing networks in brains and computer circuits. *PLoS Comput. Biol.* 6:e1000748

Bassett DS, Meyer-Lindenberg A, Achard S, Duke T, Bullmore E. 2006. Adaptive reconfiguration of fractal small-world human brain functional networks. *Proc. Natl. Acad. Sci. USA* 103:19518–23

Bernasconi C, König P. 1999. On the directionality of cortical interactions studied by structural analysis of electrophysiological recordings. *Biol. Cybern.* 81:199–210

Blondel VD, Guillaume JL, Lambiotte R, Lefebvre E. 2008. Fast unfolding of communities in large networks. *J. Stat. Mech.* 10:P10008

Bollobás B. 1985. *Random Graphs*. Cambridge, UK: Cambridge Univ. Press

Classical textbook on graph theory.

Broder A, Kumar R, Maghoul F, Raghavan P, Rajagopalan S, et al. 2000. Graph structure in the Web. *Comput. Netw.* 33:309–20

Büchel C, Friston KJ. 1997. Modulation of connectivity in visual pathways by attention: cortical interactions evaluated with structural equation modelling and fMRI. *Cereb. Cortex* 7:768–78

Buckner RL, Sepulcre J, Taludkar T, Krienen FM, Liu H, et al. 2009. Cortical hubs revealed by intrinsic functional connectivity: mapping, assessment of stability, and relation to Alzheimer's disease. *J. Neurosci.* 29:1860–73

Bullmore E, Fadili J, Maxim V, Sendur L, Whitcher B, et al. 2004. Wavelets and functional magnetic resonance imaging of the human brain. *Neuroimage* 23:S234–49

Bullmore E, Suckling J, Overmeyer S, Rabe-Hesketh S, Taylor E, Brammer M. 1999. Global, voxel, and cluster tests, by theory and permutation, for a difference between two groups of structural MR images of the brain. *IEEE Trans. Med. Imaging* 18:32–42

Bullmore ET, Barnes A, Bassett DS, Fornito A, Kitzbichler MJ, et al. 2009. Generic aspects of complexity in brain imaging data and other biological systems. *Neuroimage* 47:1125–34

Bullmore ET, Sporns O. 2009. Complex brain networks: graph theoretical analysis of structural and functional systems. *Nat. Rev. Neurosci.* 10:186–98

Comprehensive review of complex network analysis in neuroscience.

Butts CT. 2008. Social network analysis: a methodological introduction. *Asian J. Soc. Psychol.* 11:13–41

Butts CT. 2009. Revisiting the foundations of network analysis. *Science* 325:414–16

Catani M, ffytche DH. 2005. The rises and falls of disconnection syndromes. *Brain* 128:2224–39

Chen BL, Hall DH, Chklovskii DB. 2006. Wiring optimization can relate neuronal structure and function. *Proc. Natl. Acad. Sci. USA* 103:4723–28

Chen R, Herskovits EH. 2007. Graphical model-based multivariate analysis of functional magnetic resonance data. *Neuroimage* 35:635–47

Chen ZJ, He Y, Rosa-Neto P, Germann J, Evans AC. 2008. Revealing modular architecture of human brain structural networks by using cortical thickness from MRI. *Cereb. Cortex* 18:2374–81

Cheyne D, Bakhtazad L, Gaetz W. 2006. Spatiotemporal mapping of cortical activity accompanying voluntary movements using an event-related beamforming approach. *Hum. Brain Mapp.* 27:213–29

Costa LF, Rodrigues FA, Travieso G, Villas Boas PR. 2007. Characterization of complex networks: a survey of measurements. *Adv. Phys.* 56:167–242

Courchesne E, Pierce K. 2005. Why the frontal cortex in autism might be talking only to itself: local over-connectivity but long-distance disconnection. *Curr. Opin. Neurobiol.* 15:225–30

Crucitti P, Latora V, Porta S. 2006. Centrality measures in spatial networks of urban streets. *Phys. Rev. E Stat. Nonlin. Soft Matter Phys.* 73:036125

David O, Cosmelli D, Friston KJ. 2004. Evaluation of different measures of functional connectivity using a neural mass model. *Neuroimage* 21:659–73

de Haan W, Pijnenburg YA, Strijers RL, Van Der Made Y, Van Der Flier WM, et al. 2009. Functional neural network analysis in frontotemporal dementia and Alzheimer's disease using EEG and graph theory. *BMC Neurosci.* 10:101

de Vico Fallani F, Astolfi L, Cincotti F, Mattia D, la Rocca D, et al. 2009. Evaluation of the brain network organization from EEG signals: a preliminary evidence in stroke patient. *Anat. Rec. (Hoboken)* 292:2023–31

de Vico Fallani F, Astolfi L, Cincotti F, Mattia D, Marciani MG, et al. 2008a. Cortical network dynamics during foot movements. *Neuroinformatics* 6:23–34

de Vico Fallani F, Sinatra R, Astolfi L, Mattia D, Cincotti F, et al. 2008b. Community structure of cortical networks in spinal cord injured patients. *Conf. Proc. IEEE Eng. Med. Biol. Soc.* 2008:3995–98

Dehaene S, Naccache L. 2001. Towards a cognitive neuroscience of consciousness: basic evidence and a workspace framework. *Cognition* 79:1–37

Deuker L, Bullmore ET, Smith M, Christensen S, Nathan PJ, et al. 2009. Reproducibility of graph metrics of human brain functional networks. *Neuroimage* 47:1460–68

Eguíluz VM, Chialvo DR, Cecchi GA, Baliki M, Apkarian AV. 2005. Scale-free brain functional networks. *Phys. Rev. Lett.* 94:018102

Erdös P, Rényi A. 1959. On random graphs: I. *Publ. Math.* 6:290–97

Fair DA, Schlaggar BL, Cohen AL, Miezin FM, Dosenbach NU, et al. 2007. A method for using blocked and event-related fMRI data to study "resting state" functional connectivity. *Neuroimage* 35:396–405

Fodor JA. 1983. *The Modularity of Mind*. Cambridge, MA: MIT Press

Freeman LC. 1977. A set of measures of centrality based on betweenness. *Sociometry* 40:35–41

Friston K. 1994. Functional and effective connectivity in neuroimaging: a synthesis. *Hum. Brain Mapp.* 2:56–78

Friston KJ, Frith CD. 1995. Schizophrenia: a disconnection syndrome? *Clin. Neurosci.* 3:89–97

Friston KJ, Harrison L, Penny W. 2003. Dynamic causal modelling. *Neuroimage* 19:1273–302

Genovese CR, Lazar NA, Nichols T. 2002. Thresholding of statistical maps in functional neuroimaging using the false discovery rate. *Neuroimage* 15:870–78

Gong G, He Y, Concha L, Lebel C, Gross DW, et al. 2008. Mapping anatomical connectivity patterns of human cerebral cortex using in vivo diffusion tensor imaging tractography. *Cereb. Cortex* 19:524–36

Gong G, Rosa-Neto P, Carbonell F, Chen ZJ, He Y, Evans AC. 2009. Age- and gender-related differences in the cortical anatomical network. *J. Neurosci.* 29:15684–93

Guimera R, Sales-Pardo M, Amaral LA. 2007. Classes of complex networks defined by role-to-role connectivity profiles. *Nat. Phys.* 3:63–69

Hagmann P, Cammoun L, Gigandet X, Gerhard S, Ellen Grant P, et al. 2010. MR connectomics: principles and challenges. *J. Neurosci. Methods.* Epub ahead of print

Early graphical analysis of the anatomical connectome as measured by diffusion imaging.

Hagmann P, Cammoun L, Gigandet X, Meuli R, Honey CJ, et al. 2008. Mapping the structural core of human cerebral cortex. *PLoS Biol.* 6:e159

He Y, Chen ZJ, Evans AC. 2007. Small-world anatomical networks in the human brain revealed by cortical thickness from MRI. *Cereb. Cortex* 17:2407–19

He Y, Chen ZJ, Evans AC. 2008. Structural insights into aberrant topological patterns of large-scale cortical networks in Alzheimer's disease. *J. Neurosci.* 28:4756–66

He Y, Dagher A, Chen Z, Charil A, Zijdenbos A, et al. 2009a. Impaired small-world efficiency in structural cortical networks in multiple sclerosis associated with white matter lesion load. *Brain* 132:3366–79

He Y, Dagher A, Chen Z, Charil A, Zijdenbos A, et al. 2009b. Uncovering intrinsic modular organization of spontaneous brain activity in humans. *PLoS One* 4:e5226

Important early description of clustered anatomical connectivity in nonhuman brains.

Hilgetag CC, Burns GA, O'Neill MA, Scannell JW, Young MP. 2000. Anatomical connectivity defines the organization of clusters of cortical areas in the macaque monkey and the cat. *Philos. Trans. R. Soc. London B Biol. Sci.* 355:91–110

Honey C, Sporns O. 2008. Dynamical consequences of lesions in cortical networks. *Hum. Brain Mapp.* 29:802–9

Honey C, Sporns O, Cammoun L, Gigandet X, Thiran JP, et al. 2009. Predicting human resting-state functional connectivity from structural connectivity. *Proc. Natl. Acad. Sci. USA* 106:2035–40

Horstmann MT, Bialonski S, Noennig N, Mai H, Prusseit J, et al. 2010. State dependent properties of epileptic brain networks: comparative graph-theoretical analyses of simultaneously recorded EEG and MEG. *Clin. Neurophysiol.* 121:172–85

Humphries MD, Gurney K, Prescott TJ. 2006. The brainstem reticular formation is a small-world, not scale-free, network. *Proc. Biol. Sci. B* 273:503–11

Iturria-Medina Y, Canales-Rodríguez EJ, Melie-García L, Valdés-Hernández PA, Martínez-Montes E, et al. 2007. Characterizing brain anatomical connections using diffusion weighted MRI and graph theory. *Neuroimage* 36:645–60

Kaiser M, Hilgetag CC. 2006. Non-optimal component placement, but short processing paths, due to long-distance projections in neural systems. *PLoS Comput. Biol.* 2:e95

Kenny S, Andric M, Boker SM, Neale MC, Wilde M, Small SL. 2009. Parallel workflows for data-driven structural equation modeling in functional neuroimaging. *Front. Neuroinformatics* 3:34

Kitzbichler MG, Smith ML, Christensen SR, Bullmore E. 2009. Broadband criticality of human brain network synchronization. *PLoS Comput. Biol.* 5:e1000314

Knock SA, McIntosh AR, Sporns O, Kötter R, Hagmann P, Jirsa VK. 2009. The effects of physiologically plausible connectivity structure on local and global dynamics in large scale brain models. *J. Neurosci. Methods* 183:86–94

Kowalik ZJ, Elbert T. 1994. Changes of chaoticness in spontaneous EEG/MEG. *Integr. Physiol. Behav. Sci.* 29:270–82

Latora V, Marchiori M. 2001. Efficient behavior of small-world networks. *Phys. Rev. Lett.* 87:198701

Latora V, Marchiori M. 2003. Economic small-world behavior in weighted networks. *Eur. Phys. J. B* 32:249–263

Lee JH, Durand R, Gradinaru V, Zhang F, Goshen I, et al. 2010. Global and local fMRI signals driven by neurons defined optogenetically by type and wiring. *Nature* 465:788–92

Leicht EA, Newman MEJ. 2008. Community structure in directed networks. *Phys. Rev. Lett.* 100:118703

Leistedt SJ, Coumans N, Dumont M, Lanquart JP, Stam CJ, Linkowski P. 2009. Altered sleep brain functional connectivity in acutely depressed patients. *Hum. Brain Mapp.* 30:2207–19

Lerch JP, Worsley K, Shaw GP, Greenstein DK, Lenroot RK, et al. 2006. Mapping anatomical correlations across cerebral cortex (MACACC) using cortical thickness from MRI. *Neuroimage* 31:993–1003

Liu Y, Liang M, Zhou Y, He Y, Hao Y, et al. 2008. Disrupted small-world networks in schizophrenia. *Brain* 131:945–61

Li Y, Liu Y, Li J, Qin W, Li K, et al. 2009. Brain anatomical networks and intelligence. *PLoS Comput. Biol.* 5:e1000395

Lohmann G, Margulies DS, Horstmann A, Pleger B, Lepsien J, et al. 2010. Eigenvector centrality mapping for analyzing connectivity patterns in fMRI data of the human brain. *PLoS One* 5:e10232

Lynall ME, Bassett DS, Kerwin RW, McKenna PJ, Kitzbichler M, et al. 2010. Functional connectivity and brain networks in schizophrenia. *J. Neurosci.* 30:9477–87

Maslov S, Sneppen K. 2002. Specificity and stability in topology of protein networks. *Science* 296:910–13

Mechelli A, Friston KJ, Frackowiak RS, Price CJ. 2005. Structural covariance in the human cortex. *J. Neurosci.* 25:8303–10

Meunier D, Achard S, Morcom A, Bullmore E. 2008. Age-related changes in modular organization of human brain functional networks. *Neuroimage* 44:715–23

Meunier D, Lambiotte R, Fornito A, Ersche KD, Bullmore ET. 2009. Hierarchical modularity in human brain functional networks. *Front. Neuroinformatics* 3:37

Micheloyannis S, Pachou E, Stam CJ, Breakspear M, Bitsios P, et al. 2006. Small-world networks and disturbed functional connectivity in schizophrenia. *Schizophr. Res.* 87:60–66

Micheloyannis S, Vourkas M, Tsirka V, Karakonstantaki E, Kanatsouli K, Stam CJ. 2009. The influence of ageing on complex brain networks: a graph theoretical analysis. *Hum. Brain Mapp.* 30:200–8

Murphy K, Birn RM, Handwerker DA, Jones TB, Bandettini PA. 2009. The impact of global signal regression on resting state correlations: Are anti-correlated networks introduced? *Neuroimage* 44:893–905

Newman MEJ. 2006. Modularity and community structure in networks. *Proc. Natl. Acad. Sci. USA* 103:8577–82
Niven JE, Laughlin SB. 2008. Energy limitation as a selective pressure on the evolution of sensory systems. *J. Exp. Biol.* 211:1792–804
Oldham MC, Horvath S, Geschwind DH. 2006. Conservation and evolution of gene coexpression networks in human and chimpanzee brains. *Proc. Natl. Acad. Sci. USA* 103:17973–78
Palva JM, Monto S, Kulashekar S, Palva S. 2010a. Neuronal synchrony reveals working memory networks and predicts individual memory capacity. *Proc. Natl. Acad. Sci. USA* 107:7580–85
Palva S, Monto S, Palva JM. 2010b. Graph properties of synchronized cortical networks during visual working memory maintenance. *Neuroimage* 49:3257–68
Park CH, Kim SY, Kim YH, Kim K. 2008. Comparison of the small-world topology between anatomical and functional connectivity in the human brain. *Physica A* 387:5958–62
Poldrack RA, Fletcher PC, Henson RN, Worsley KJ, Brett M, Nichols TE. 2008. Guidelines for reporting an fMRI study. *Neuroimage* 40:409–14
Ponten SC, Bartolomei F, Stam CJ. 2007. Small-world networks and epilepsy: graph theoretical analysis of intracerebrally recorded mesial temporal lobe seizures. *Clin. Neurophysiol.* 118:918–27
Ponten SC, Douw L, Bartolomei F, Reijneveld JC, Stam CJ. 2009. Indications for network regularization during absence seizures: weighted and unweighted graph theoretical analyses. *Exp. Neurol.* 217:197–204
Raj A, Mueller SG, Young K, Laxer KD, Weiner M. 2010. Network-level analysis of cortical thickness of the epileptic brain. *Neuroimage* 52:1302–13
Richiardi J, Eryilmaz H, Schwartz S, Vuilleumier P, Van De Ville D. 2010. Decoding brain states from fMRI connectivity graphs. *Neuroimage.* Epub ahead of print
Robinson PA, Henderson JA, Matar E, Riley P, Gray RT. 2009. Dynamical reconnection and stability constraints on cortical network architecture. *Phys. Rev. Lett.* 103:108104
Rubinov M, Knock SA, Stam CJ, Micheloyannis S, Harris AWF, et al. 2009. Small-world properties of nonlinear brain activity in schizophrenia. *Hum. Brain Mapp.* 30:403–16

Comprehensive description of graph metrics in neuroscience.

Rubinov M, Sporns O. 2010. Complex network measures of brain connectivity: uses and interpretations. *Neuroimage* 52:1059–69
Salvador R, Martínez A, Pomarol-Clotet E, Gomar J, Vila F, et al. 2008. A simple view of the brain through a frequency-specific functional connectivity measure. *Neuroimage* 39:279–89
Salvador R, Suckling J, Coleman MR, Pickard JD, Menon D, Bullmore E. 2005a. Neurophysiological architecture of functional magnetic resonance images of human brain. *Cereb. Cortex* 15:1332–42
Salvador R, Suckling J, Schwarzbauer C, Bullmore E. 2005b. Undirected graphs of frequency-dependent functional connectivity in whole brain networks. *Philos. Trans. R. Soc. London B Biol. Sci.* 360:937–46
Scannell JW, Blakemore C, Young MP. 1995. Analysis of connectivity in the cat cerebral cortex. *J. Neurosci.* 15:1463–83
Scannell JW, Burns GA, Hilgetag CC, O'Neil MA, Young MP. 1999. The connectional organization of the cortico-thalamic system of the cat. *Cereb. Cortex* 9:277–99
Schmitt JE, Lenroot RK, Wallace GL, Ordaz S, Taylor KN, et al. 2008. Identification of genetically mediated cortical networks: a multivariate study of pediatric twins and siblings. *Cereb. Cortex* 18:1737–47
Schwarz AJ, Gozzi A, Bifone A. 2009. Community structure in networks of functional connectivity: resolving functional organization in the rat brain with pharmacological MRI. *Neuroimage* 47:302–11
Shu N, Liu Y, Li J, Li Y, Yu C, Jiang T. 2009. Altered anatomical network in early blindness revealed by diffusion tensor tractography. *PLoS One* 4:e7228

Prescient essay on nearly decomposable information-processing systems.

Simon H. 1962. The architecture of complexity. *Proc. Am. Philos. Soc.* 106:467–82
Skudlarski P, Jagnnathan K, Calhoun VD, Hampson M, Skudlarski BA, Pearlson G. 2008. Measuring brain connectivity: Diffusion tensor imaging validates resting state temporal correlations. *Neuroimage* 43:554–61
Smit DJ, Stam CJ, Posthuma D, Boomsma DI, de Geus EJ. 2008. Heritability of "small-world" networks in the brain: a graph theoretical analysis of resting-state EEG functional connectivity. *Hum. Brain Mapp.* 29:1368–78
Smith SM, Miller KL, Salimi-Khorshidi G, Webster M, Beckmann CF. 2010. Network modeling methods for fMRI. *Neuroimage.* Epub ahead of print

Sporns O. 2010. *Networks of the Brain*. Cambridge, MA: MIT Press
Sporns O, Chialvo DR, Kaiser M, Hilgetag CC. 2004. Organization, development and function of complex brain networks. *Trends Cogn. Sci.* 8:418–25
Sporns O, Honey CJ, Kotter R. 2007. Identification and classification of hubs in brain networks. *PLoS One* 2:e1049
Sporns O, Tononi G, Kötter R. 2005. The human connectome: a structural description of the human brain. *PLoS Comput. Biol.* 1:e42
Stam CJ. 2004. Functional connectivity patterns of human magnetoencephalographic recordings: a "small-world" network? *Neurosci. Lett.* 355:25–28
Stam CJ. 2010. Use of magnetoencephalography (MEG) to study functional brain networks in neurodegenerative disorders. *J. Neurol. Sci.* 289:128–34
Stam CJ, Jones BF, Nolte G, Breakspear M, Scheltens P. 2007a. Small-world networks and functional connectivity in Alzheimer's disease. *Cereb. Cortex* 17:92–99
Stam CJ, Nolte G, Daffertshofer A. 2007b. Phase lag index: assessment of functional connectivity from multi-channel EEG and MEG with diminished bias from common sources. *Hum. Brain Mapp.* 28:1178–93
Strogatz SH. 2001. Exploring complex networks. *Nature* 410:268–76
Supekar K, Menon V, Rubin D, Musen M, Greicius MD. 2008. Network analysis of intrinsic functional brain connectivity in Alzheimer's disease. *PLoS Comput. Biol.* 4:e1000100
Tononi G, Sporns O, Edelman GM. 1994. A measure for brain complexity: relating functional segregation and integration in the nervous system. *Proc. Natl. Acad. Sci. USA* 91:5033–37
Tzourio-Mazoyer N, Landeau B, Papathanassiou D, Crivello F, Etard O, et al. 2002. Automated anatomical labelling of activations in SPM using a macroscopic anatomical parcellation of the MNI MRI single-subject brain. *Neuroimage* 15:273–79
van Dellen E, Douw L, Baayen JC, Heimans JJ, Ponten SC, et al. 2009. Long-term effects of temporal lobe epilepsy on local neural networks: a graph theoretical analysis of corticography recordings. *PLoS One* 4:e8081
van den Heuvel MP, Stam CJ, Boersma M, Hulshoff Pol HE. 2008. Small-world and scale-free organization of voxel-based resting-state functional connectivity in the human brain. *Neuroimage* 43:528–39
van den Heuvel MP, Stam CJ, Kahn RS, Hulshoff Pol HE. 2009. Efficiency of functional brain networks and intellectual performance. *J. Neurosci.* 29:7619–24
Van Dijk KRE, Hedden T, Venkataraman A, Evans KC, Lazar SW, Buckner RL. 2010. Intrinsic functional connectivity as a tool for human connectomics: theory, properties, and optimization. *J. Neurophysiol.* 103:297–321
Vrba J, Robinson SE. 2001. Signal processing in magnetoencephalography. *Methods* 25:249–71
Wang J, Zuo X, He Y. 2009. Parcellation-dependent small-world brain functional networks: a resting-state fMRI study. *Hum. Brain Mapp.* 30:1511–23
Wang J, Zuo X, He Y. 2010. Graph-based network analysis of resting-state functional MRI. *Front. Syst. Neurosci.* 4:16
Wang L, Zhu C, He Y, Zang Y, Cao Q, et al. 2008. Altered small-world brain functional networks in children with attention-deficit/hyperactivity disorder. *Hum. Brain Mapp.* 30:638–49
Watts DJ, Strogatz SH. 1998. Collective dynamics of "small-world" networks. *Nature* 393:440–42
Weissenbacher A, Kasess C, Gerstl F, Lanzenberger R, Moser E, Windischberger C. 2009. Correlations and anticorrelations in resting-state functional connectivity MRI: a quantitative comparison of preprocessing strategies. *Neuroimage* 47:1408–16
White JG, Southgate E, Thomson JN, Brenner S. 1986. The structure of the nervous system of the nematode *Caenorhabditis elegans*. *Philos. Trans. R. Soc. London B* 314:1–340
Whitfield-Gabrieli S, Thermenos HW, Milanovic S, Tsuang MT, Faraone SV, et al. 2009. Hyperactivity and hyperconnectivity of the default network in schizophrenia and in first-degree relatives of persons with schizophrenia. *Proc. Natl. Acad. Sci. USA* 106:1279–84
Wright IC, Sharma T, Ellison ZR, McGuire PK, Friston KJ, et al. 1999. Supraregional brain systems and the neuropathology of schizophrenia. *Cereb. Cortex* 9:366–78

Yoon JH, Minzenberg MJ, Ryan Walter BS, Wendelken C, Ragland JD, Carter CS. 2008. Association of dorsolateral prefrontal cortex dysfunction with disrupted coordinated brain activity in schizophrenia: relationship with impaired cognition, behavioral disorganization, and global function. *Am. J. Psychiatry* 165:1006–14

Young MP. 1992. Objective analysis of the topological organization of the primate cortical visual system. *Nature* 358:152–55

Young MP. 1993. The organization of neural systems in the primate cerebral cortex. *Proc. Biol. Sci.* 252:13–18

Yu S, Huang D, Singer W, Nikolic D. 2008. A small world of neuronal synchrony. *Cereb. Cortex* 18:2891–901

Zalesky A, Fornito A. 2009. A DTI-derived measure of cortico-cortical connectivity. *IEEE Trans. Med. Imag.* 28:1023–36

Zalesky A, Fornito A, Bullmore E. 2010a. Network-based statistic: identifying differences in brain networks. *Neuroimage* 53:1197–207

Zalesky A, Fornito A, Harding IH, Cocchi L, Yücel M, et al. 2010b. Whole-brain anatomical networks: Does the choice of nodes matter? *Neuroimage* 50:970–83

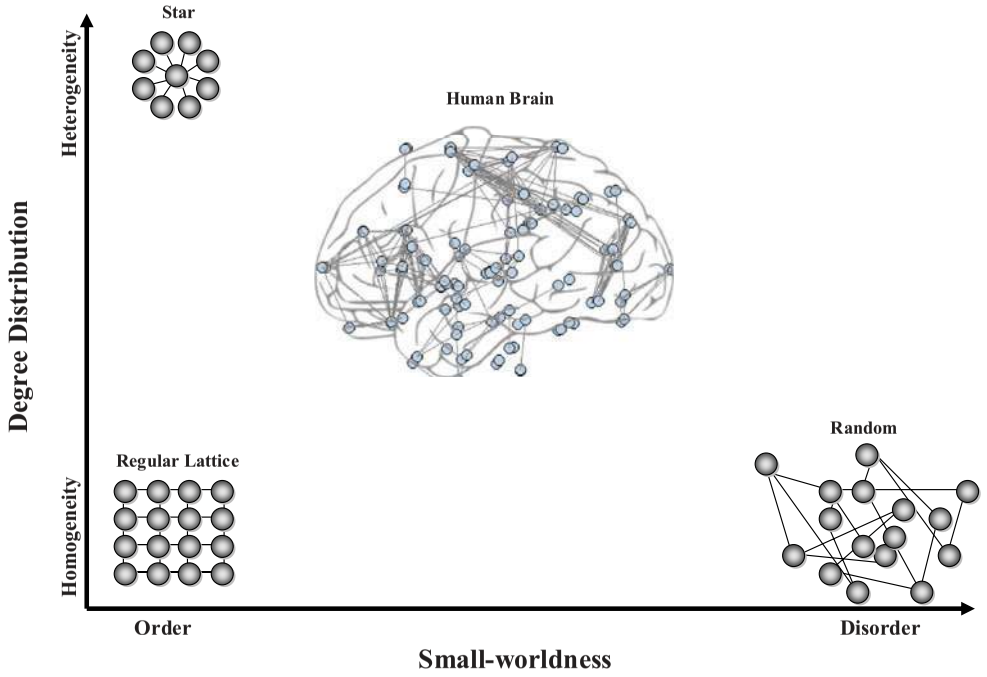

Figure 1

Organization of human brain networks in comparison to extremal architectures on topological dimensions of small-worldness (*x*-axis) and degree distribution (*y*-axis). Small-world networks, like the brain, exist between the extreme boundaries of a regular lattice network (*lower left*) and pure random network (*lower right*). Random and regular networks, although differing in terms of order/disorder, both have homogeneous degree distributions; that is, all nodes are connected to roughly the same number of other nodes. In contrast, a star network (*upper left*) is maximally heterogeneous, with a single high-degree hub and many low-degree peripheral nodes. The human brain network, as measured by both structural and functional neuroimaging, lies in between these two extremes and displays a broad-scale degree distribution where low-degree nodes, medium-degree nodes, and high-degree nodes coexist in unison and collectively form the network architecture. This heterogeneity is the necessary substrate for nodes to perform a broad range of functional roles. Circles indicate regional nodes of the brain network; gray lines indicate connections between them. Edges connecting nodes are unweighted or binary (they are either present or not present) and undirected (if an edge links node *i* to node *j*, it also links node *j* to node *i*).

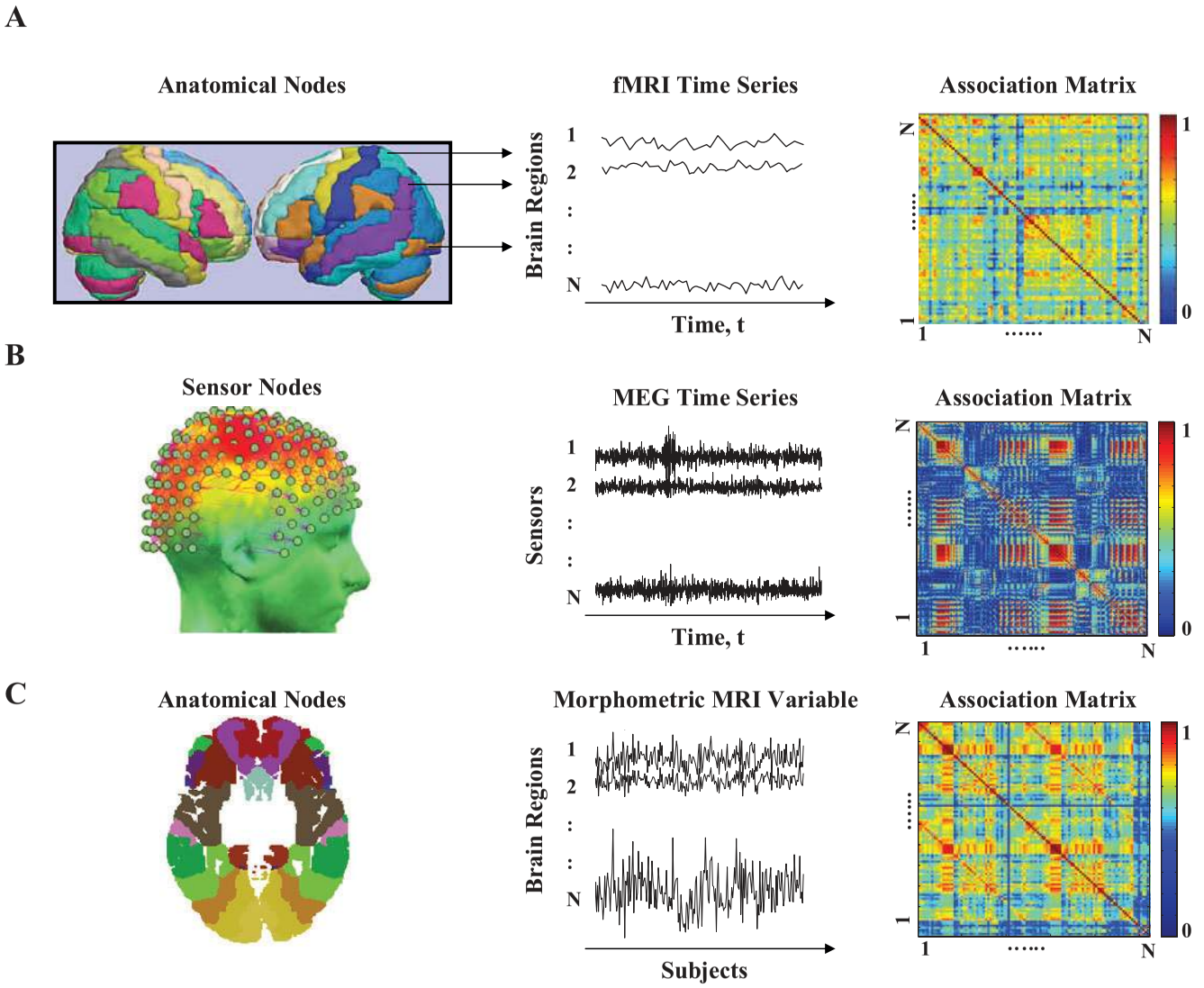

Figure 2

From data to association matrix. (*A*) An anatomical template image (*left*) is used to parcellate the voxel-level fMRI data. Regional mean time series (*middle*) are estimated for each of the N = 90 regions in the parcellation template. The pair-wise association $a_{i,j}$ is estimated between the *i*th and *j*th nodes, $i \neq j = 1, 2, 3, \ldots, N$ and compiled for all possible pairs to form a $\{N \times N\}$ interregional association matrix, *A* (*right*). If we choose the measure of association to be the absolute Pearson's correlation between two time series, then this value ranges between 0 and 1. (*B*) For EEG or MEG data, neurophysiological time series are measured by an array of sensors (*left*), each of which provides a nodal time series (*middle*) at frequencies generally higher than those measured by fMRI. Due to this increase in temporal resolution, a wide variety of association metrics can be applied, including mutual information, synchronization, and phase coherence (*right*), to construct an association matrix. (*C*) Several morphometric variables can be computed on a regional basis (*left*) from individual structural MRI images, including gray matter volume, cortical thickness, surface area, and curvature (*middle*). The correlation or partial correlation of these regional morphometric variables over subjects provides an association matrix (*right*), which can be used as a measure of anatomical connectivity (Lerch et al. 2006).

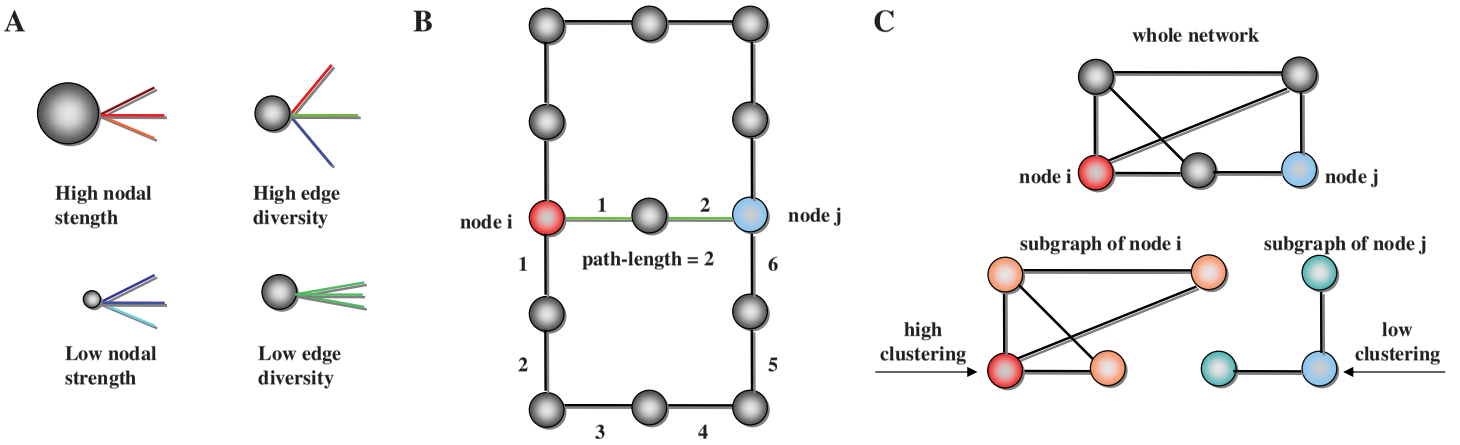

Figure 3

Schematic definitions of basic connectivity and graph metrics. (*A*) Nodal strength is the sum of the associations between the index node and all other nodes in the system, and edge diversity is defined as the standard deviation of the associations. The magnitude of association is given by the color of the lines, where red indicates a strong association and blue indicates a weak association; the strength of a node is represented as proportional to its size. (*B*) Path length. The path length from node *i* (shown in red) to node *j* (shown in blue) is defined as the fewest number of edges that must be traversed to get from node *i* to node *j*. In this case, the minimum path length is 2 (shown in green). There may be longer paths available (such as the path of length 6 shown in gray around the bottom loop of the network). The path length of a network is inversely proportional to its efficiency of parallel information transfer. (*C*) Clustering coefficient is a measure of local connectivity and is highly correlated with the local efficiency of information transfer (Latora & Marchiori 2001). We show a toy network (*top*) and determine the clustering of node *i* (shown in red) and node *j* (shown in blue). The nearest neighbors of the highly clustered node *i* are connected to each other, to form triangle motifs, whereas the nearest neighbors of the less clustered node *j* are not connected to each other.

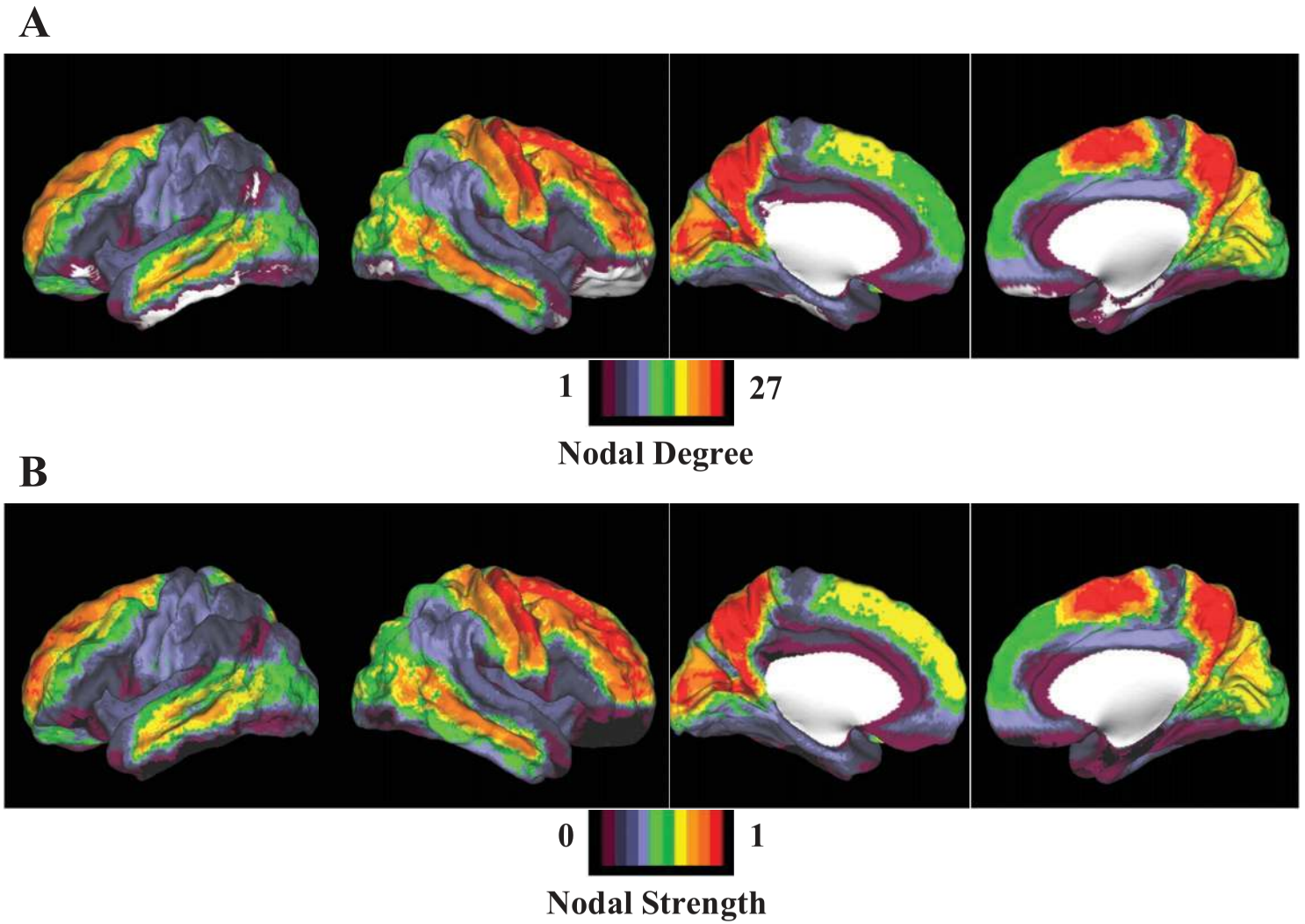

Figure 4

Convergent aspects of functional connectivity and functional network analysis. (*A*) Cortical surface maps showing the spatial distribution of nodal degree in a single fMRI dataset. Warm colors indicate high degree, cool colors indicate low degree, and white indicates regions that are disconnected from the graph. (*B*) Cortical surface maps showing the spatial distribution of nodal strength for the same fMRI dataset, where again warm colors indicate a high nodal strength and cool colors indicate a low nodal strength. The comparison of *A* and *B* highlights the similarity between nodal degree and nodal strength present in many networks derived from functional neuroimaging data.

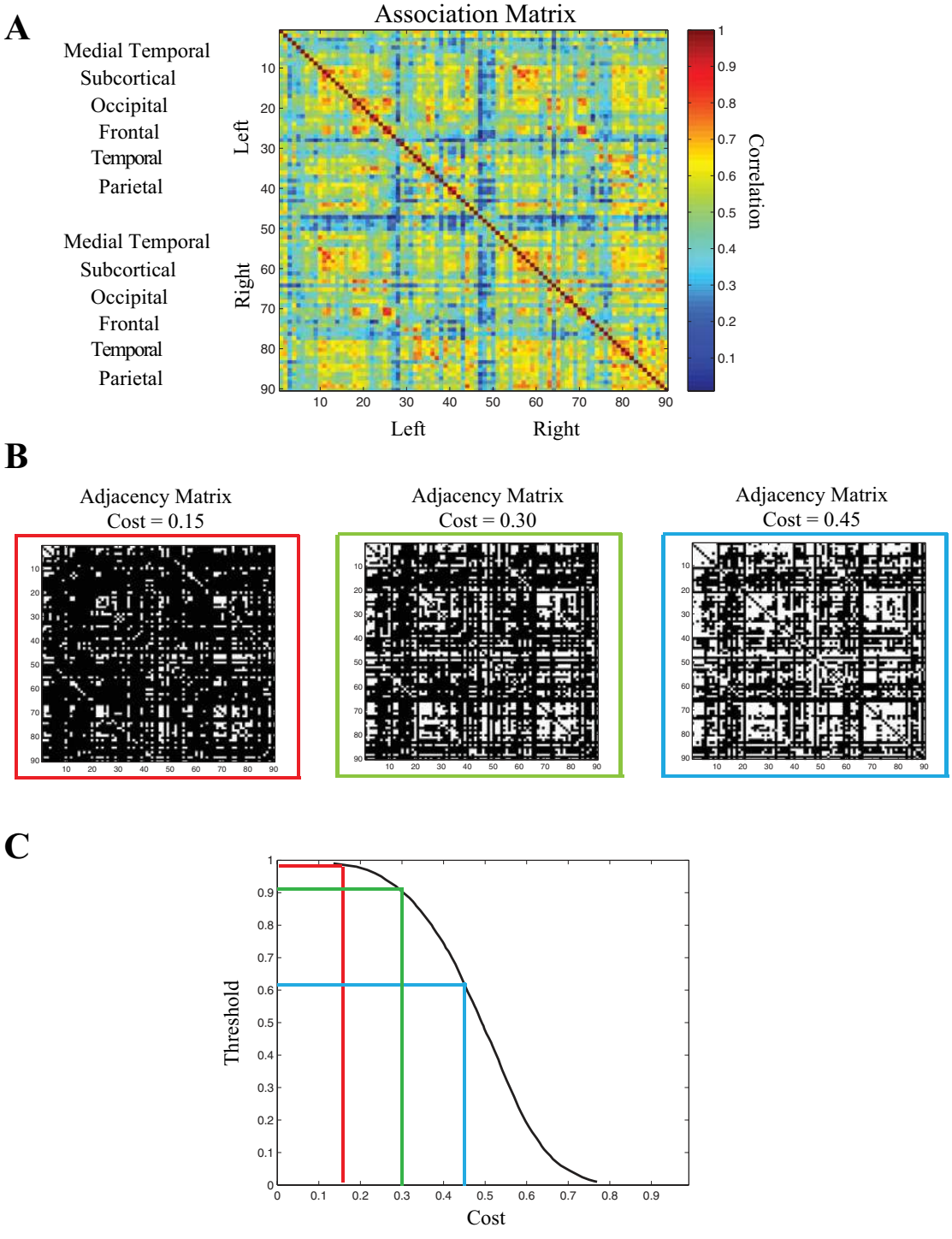

Figure 5

From association matrix to adjacency matrix. (*A*) The association matrix represents the absolute value of all pair-wise wavelet correlations estimated for a single fMRI dataset (see Achard et al. 2006). The 90 nodal regions of the Automated Anatomical Labeling (AAL) template are ordered into left and right hemispheres, and then into six anatomical clusters (medial temporal, subcortical, occipital, frontal, temporal, parietal) as defined by Salvador et al. (2005a). (*B*) The three adjacency matrices shown were obtained by thresholding the association matrix in *A* at costs of $\kappa = 0.15$ (*left*), $\kappa = 0.30$ (*middle*), and $\kappa = 0.45$ (*right*). White elements in the adjacency matrices indicate the existence of an edge, and black elements indicate the absence of an edge. Note that the density of connections or topological cost of the matrix increases with decreasing threshold. (*C*) Plot of the connection density or cost (*x*-axis) as a function of the threshold applied to the association matrix (*y*-axis) to construct the adjacency matrix; association matrices thresholded at higher values will have fewer edges than those thresholded at lower values. Colored lines in the plot indicate the costs at which the three adjacency matrices shown in *B* were calculated.

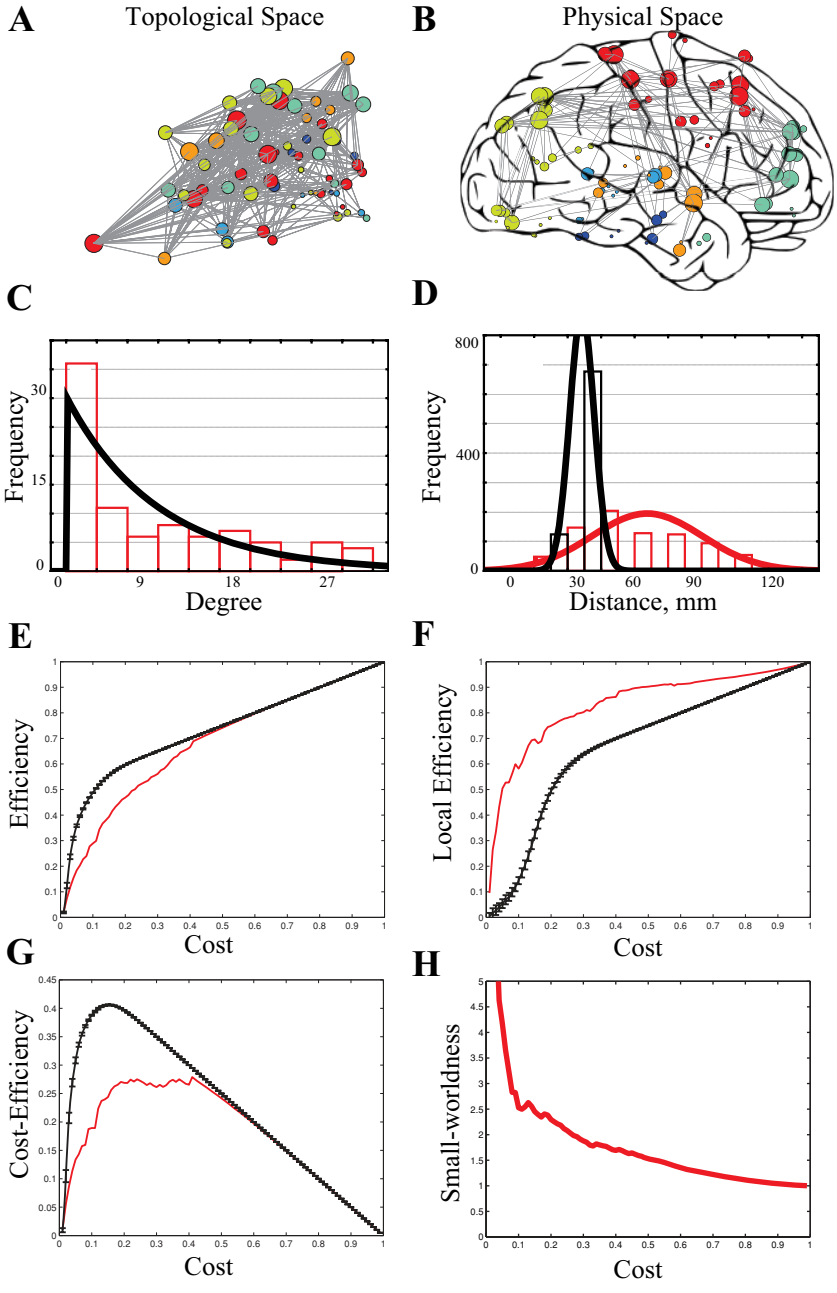

Figure 6

Topological and geometrical properties of functional brain graphs. (*A*) For a single fMRI dataset, we calculated the adjacency matrix at a cost of $\kappa = 0.05$, and the edges present in this adjacency matrix were plotted here in topological space so that the distance between nodes is larger if those nodes are separated by a longer path length and smaller if they are separated by a shorter topological path length. The size of nodes indicates nodal degree whereas the color of the node indicates its lobar identity. (*B*) Brain graph plotted in physical space where the distance between nodes is the Euclidean distance between regional centroids in the anatomical space of the real brain. The size of nodes indicates nodal degree whereas the color of the node indicates its lobar identity. (*C*) Plot of the degree distribution (*red*) and distribution fit (*black*) of the brain graph, showing the predominance of low-degree nodes and the presence of a few high-degree hubs. (*D*) Plot of the distribution of physical distance of connections of the brain graph (*red*) in comparison to the distance distribution in a minimally rewired network (*black*). (*E*) Plot of global efficiency versus cost for the brain network (*red*) and a distribution of 100 comparable random networks (*black*). (*F*) Plot of local efficiency versus cost for the brain network (*red*) and a distribution of 100 comparable random networks (*black*). (*G*) Plot of the cost-efficiency versus cost for the brain network (*red*) and a distribution of 100 comparable random networks (*black*). (*H*) Plot of small-worldness versus cost for the brain network (*red*). The small-worldness scalar $\sigma = 1$ in a random graph.

Annual Review of
Clinical Psychology

Volume 7, 2011

Contents

The Origins and Current Status of Behavioral Activation Treatments for Depression
Sona Dimidjian, Manuel Barrera Jr., Christopher Martell, Ricardo F. Muñoz, and Peter M. Lewinsohn 1

Animal Models of Neuropsychiatric Disorders
A.B.P. Fernando and T.W. Robbins 39

Diffusion Imaging, White Matter, and Psychopathology
Moriah E. Thomason and Paul M. Thompson 63

Outcome Measures for Practice
Jason L. Whipple and Michael J. Lambert 87

Brain Graphs: Graphical Models of the Human Brain Connectome
Edward T. Bullmore and Danielle S. Bassett 113

Open, Aware, and Active: Contextual Approaches as an Emerging Trend in the Behavioral and Cognitive Therapies
Steven C. Hayes, Matthieu Villatte, Michael Levin, and Mikaela Hildebrandt 141

The Economic Analysis of Prevention in Mental Health Programs
Cathrine Mihalopoulos, Theo Vos, Jane Pirkis, and Rob Carter 169

The Nature and Significance of Memory Disturbance in Posttraumatic Stress Disorder
Chris R. Brewin 203

Treatment of Obsessive Compulsive Disorder
Martin E. Franklin and Edna B. Foa 229

Acute Stress Disorder Revisited
Etzel Cardeña and Eve Carlson 245

Personality and Depression: Explanatory Models and Review of the Evidence
Daniel N. Klein, Roman Kotov, and Sara J. Bufferd 269

Sleep and Circadian Functioning: Critical Mechanisms in the Mood Disorders?
Allison G. Harvey 297

Personality Disorders in Later Life: Questions About the Measurement, Course, and Impact of Disorders
Thomas F. Oltmanns and Steve Balsis 321

Efficacy Studies to Large-Scale Transport: The Development and Validation of Multisystemic Therapy Programs
Scott W. Henggeler 351

Gene-Environment Interaction in Psychological Traits and Disorders
Danielle M. Dick 383

Psychological Treatment of Chronic Pain
Robert D. Kerns, John Sellinger, and Burel R. Goodin 411

Understanding and Treating Insomnia
Richard R. Bootzin and Dana R. Epstein 435

Psychologists and Detainee Interrogations: Key Decisions, Opportunities Lost, and Lessons Learned
Kenneth S. Pope 459

Disordered Gambling: Etiology, Trajectory, and Clinical Considerations
Howard J. Shaffer and Ryan Martin 483

Resilience to Loss and Potential Trauma
George A. Bonanno, Maren Westphal, and Anthony D. Mancini 511

Indexes

Cumulative Index of Contributing Authors, Volumes 1–7 537

Cumulative Index of Chapter Titles, Volumes 1–7 540

Errata

An online log of corrections to *Annual Review of Clinical Psychology* articles may be found at http://clinpsy.annualreviews.org